NAVAL POSTGRADUATE SCHOOL

MONTEREY, CALIFORNIA

THESIS

STATISTICAL-DYNAMICAL FORECASTING OF TROPICAL CYCLOGENESIS IN THE NORTH ATLANTIC AT INTRASEASONAL LEAD TIMES

by

Chad S. Raynak

June 2009

Thesis Co-Advisors: Tom Murphree
David W. Meyer

Approved for public release; distribution is unlimited

THIS PAGE INTENTIONALLY LEFT BLANK

REPORT DOCUMENTATION PAGE			*Form Approved OMB No. 0704-0188*
Public reporting burden for this collection of information is estimated to average 1 hour per response, including the time for reviewing instruction, searching existing data sources, gathering and maintaining the data needed, and completing and reviewing the collection of information. Send comments regarding this burden estimate or any other aspect of this collection of information, including suggestions for reducing this burden, to Washington headquarters Services, Directorate for Information Operations and Reports, 1215 Jefferson Davis Highway, Suite 1204, Arlington, VA 22202-4302, and to the Office of Management and Budget, Paperwork Reduction Project (0704-0188) Washington DC 20503.			
1. AGENCY USE ONLY *(Leave blank)*	**2. REPORT DATE** June 2009	**3. REPORT TYPE AND DATES COVERED** Master's Thesis	
4. TITLE AND SUBTITLE Statistical-Dynamical Forecasting of Tropical Cyclogenesis in the North Atlantic at Intraseasonal Lead Times			**5. FUNDING NUMBERS**
6. AUTHOR(S) Chad S. Raynak			
7. PERFORMING ORGANIZATION NAME(S) AND ADDRESS(ES) Naval Postgraduate School Monterey, CA 93943-5000			**8. PERFORMING ORGANIZATION REPORT NUMBER**
9. SPONSORING /MONITORING AGENCY NAME(S) AND ADDRESS(ES) N/A			**10. SPONSORING/MONITORING AGENCY REPORT NUMBER**
11. SUPPLEMENTARY NOTES The views expressed in this thesis are those of the author and do not reflect the official policy or position of the Department of Defense or the U.S. Government.			
12a. DISTRIBUTION / AVAILABILITY STATEMENT Approved for public release; distribution is unlimited			**12b. DISTRIBUTION CODE**

13. ABSTRACT (maximum 200 words)

We have created a combined statistical-dynamical model to predict the probability of tropical cyclone (TC) formation at daily, 2.5° horizontal resolution in the North Atlantic (NA) at intraseasonal lead times. Based on prior research and our own analyses, we chose five large scale environmental factors (LSEFs) to represent favorable environments for TC formation. The LSEFs include: 850 mb relative vorticity, sea surface temperature, vertical wind shear, Coriolis, and 200 mb divergence. We used logistic regression to create a statistical model that depicts the probability for TC formation based on these LSEFs. Through verification of zero lead hindcasts, we determined that our regression model performs better than climatology. For example, these hindcasts had a Brier skill score of 0.04 and a relative operating characteristic skill score of 0.72. We then forced our regression model with LSEF fields from the NCEP Climate Forecast System to produce non-zero lead hindcasts and forecasts. We conducted a series of case studies to evaluate and study the predictive skill of our regression model, with the results showing that our model produces promising results at intraseasonal lead times.

14. SUBJECT TERMS Tropical Cyclones, Tropical Cyclogenesis, North Atlantic, Intraseasonal Forecasting, Smart Climatology, Tropical Genesis Parameters, Large Scale Environmental Factors, NCEP Climate Forecast System			**15. NUMBER OF PAGES** 93
			16. PRICE CODE
17. SECURITY CLASSIFICATION OF REPORT Unclassified	**18. SECURITY CLASSIFICATION OF THIS PAGE** Unclassified	**19. SECURITY CLASSIFICATION OF ABSTRACT** Unclassified	**20. LIMITATION OF ABSTRACT** UU

NSN 7540-01-280-5500

Standard Form 298 (Rev. 8-98)
Prescribed by ANSI Std. Z39.18

THIS PAGE INTENTIONALLY LEFT BLANK

Approved for public release; distribution is unlimited

STATISTICAL-DYNAMICAL FORECASTING OF TROPICAL CYCLOGENESIS IN THE NORTH ATLANTIC AT INTRASEASONAL LEAD TIMES

Chad S. Raynak
Captain, United States Air Force
B.S., Michigan State University, 2002
B.S., Naval Postgraduate School, 2004

Submitted in partial fulfillment of the
requirements for the degree of

MASTER OF ARTS OR SCIENCE IN METEOROLOGY

from the

NAVAL POSTGRADUATE SCHOOL
JUNE 2009

Author: Chad S. Raynak

Approved by: Tom Murphree
Co-Advisor

David W. Meyer
Co-Advisor

Philip A. Durkee
Chairman, Department of Meteorology

THIS PAGE INTENTIONALLY LEFT BLANK

ABSTRACT

We have created a combined statistical-dynamical model to predict the probability of tropical cyclone (TC) formation at daily, 2.5° horizontal resolution in the North Atlantic (NA) at intraseasonal lead times. Based on prior research and our own analyses, we chose five large scale environmental factors (LSEFs) to represent favorable environments for TC formation. The LSEFs include: 850 mb relative vorticity, sea surface temperature, vertical wind shear, Coriolis, and 200 mb divergence. We used logistic regression to create a statistical model that depicts the probability for TC formation based on these LSEFs. Through verification of zero lead hindcasts, we determined that our regression model performs better than climatology. For example, these hindcasts had a Brier skill score of 0.04 and a relative operating characteristic skill score of 0.72. We then forced our regression model with LSEF fields from the NCEP Climate Forecast System to produce non-zero lead hindcasts and forecasts. We conducted a series of case studies to evaluate and study the predictive skill of our regression model, with the results showing that our model produces promising results at intraseasonal lead times.

THIS PAGE INTENTIONALLY LEFT BLANK

TABLE OF CONTENTS

THIS PAGE INTENTIONALLY LEFT BLANK

LIST OF FIGURES

THIS PAGE INTENTIONALLY LEFT BLANK

LIST OF TABLES

THIS PAGE INTENTIONALLY LEFT BLANK

LIST OF ACRONYMS AND ABBREVIATIONS

14WS	14th Weather Squadron, formerly named AFCCC
AFCCC	Air Force Combat Climatology Center, now named 14WS
AFW	Air Force Weather
AIC	Akaike Information Criterion
AMIP–II	Atmospheric Model Intercomparison Project–II
BS	Brier score
BSS	Brier skill score
CFS	Climate Forecast System
CPC	Climate Prediction Center
DoD	Department of Defense
DOE	Department of Energy
ECMWF	European Centre for Medium-range Weather Forecasts
ENLN	El Niño-La Niña
EPS	Ensemble Prediction System
GCM	General circulation model
GFDL	Geophysical Fluid Dynamics Laboratory
GFS	Global Forecast System
IRI	International Research Institute for Climate and Society
JASO	July, August, September, and October
JTWC	Joint Typhoon Warning Center
LSEF	Large-scale environmental factor
LTM	Long term mean
MJO	Madden-Julian oscillation
MOM3	Modular Ocean Model version 3
MSLP	Mean sea level pressure
NAO	North Atlantic Oscillation
NCAR	National Center for Atmospheric Research

NCEP	National Centers for Environmental Prediction
NHC	National Hurricane Center
NOAA	National Oceanic and Atmospheric Administration
NTCI	Non-tropical cyclone information
OI	Optimum interpolation
OLR	Outgoing longwave radiation
R2	NCEP/DOE AMIP–II Reanalysis
ROC	Relative operating characteristic
ROCSS	Relative operating characteristic skill score
SST	Sea surface temperature
TC	Tropical cyclone
USN	United States Navy
WNP	Western North Pacific

ACKNOWLEDGMENTS

I would like to thank my thesis advisors Professors Tom Murphree and Mr. David Meyer for providing great support throughout this process. I would not be in the position to graduate without the help of my teammate, Capt. Bryan Mundhenk, whose endless patience guided me through his 2,000+ lines of MATLAB code. I would like to thank Bob Creasey for collecting and formatting the data needed for this research. Many thanks to Professor Pat Harr for guidance in all things tropical.

THIS PAGE INTENTIONALLY LEFT BLANK

I. INTRODUCTION

A. BACKGROUND

Hurricane Katrina in 2005 demonstrated the devastating force of a tropical cyclone (TC). The National Hurricane Center (NHC) estimated the death toll from Katrina at 1,833 and the property damage toll of $81 billion (NHC 2006). In 1900, the biggest natural disaster in U.S. history, the Galveston Hurricane of 1900, claimed over 8,000 lives (Emanuel 2005). Not only do TCs have an impact on civilian affairs, but they have destroyed whole militaries and with it the dreams of nations. In 1565, a TC destroyed the French fleet off the coast of St. Augustine, Florida, which forced the French to surrender Florida to Spain (Emanuel 2005).

Looking further back into history, Japan might be under Chinese rule today if not for two typhoons (Emanuel 2005). In 1274, Kublai Khan, the grandson of the infamous Genghis Khan, tried to conquer Japan for the Mongols. Kublai sent 40,000 men on 900 ships from present-day Korea to Japan. Just as the ships pulled into harbor, a typhoon hit the coast and 13,000 men perished. Yet Kublai did not learn his lesson. Just seven years later, Kublai and 140,000 men set sail to conquer Japan; however, another typhoon struck as the Japanese desperately defended the coast. Kublai himself managed to escape, but he left his men to die.

In recent history, Admiral William Halsey, Jr. made the mistake of letting not one but two typhoons taint his career. In December 1944, while the commander of the Third Fleet, Admiral Halsey decided to leave his forces in the path of Typhoon Cobra near the Philippines. Though they had time to escape the path of Cobra, three destroyers were sunk and many other vessels sustained damage due to the TC. Also, 146 aircraft were lost and more importantly over 800 seamen lost their lives due to Admiral Halsey's poor decision (Melton 2007).

One month later, Admiral Halsey again found his forces in the path of a typhoon. Although no ships were lost, six lives were lost and 75 planes were destroyed. A Navy court of inquiry convened on both occasions and found the Admiral guilty of bad judgment; however, he did not receive any punishment (Melton 2007).

For a modern day example, the United States Navy (USN) conducts an annual exercise, UNITAS gold, which is an 11-nation naval exercise in the North Atlantic (NA), conducting anti-piracy and anti-drug smuggling training. The military planners ask one to three months before the exercise, will the weather, specifically TCs, cooperate? Right now, operational forecasts of individual TCs are limited mainly to lead times of two to three days. For longer leads, the weather community generally only provides TC climatology as a guide for TC formation in the NA.

B. CLIMATE OSCILLATIONS AND IMPACTS ON TC FORMATION

TC activity undergoes large climate scale variations, for example, interannual variations in TC formations. In some years, the Gulf of Mexico has produced eight TCs, while in other years the Gulf has not produced any TCs. Having an understanding of these climate variations can lead to better TC formation forecasting because it accounts for the variability of the large scale, low frequency conditions that influence TC formation.

1. El Nino and La Nina

As described by Hilldebrand (2001), El Nino (EN) and La Nina (LN) events alter the circulations in the NA by influencing the tropical easterly jet and creating anomalous extratropical wave trains. Though ENLN have the biggest influence in the western North Pacific (WNP), they also alter the wind shear and steering flow in the NA. These circulation changes lead, on average, to more, and more intense, TCs in the NA during a LN than an EN. Also, during a LN, more TCs form in the tropical NA, while during a EN more storms form in the subtropical NA.

2. Madden-Julian Oscillation

As described by Madden and Julian (1994), the Madden Julian oscillation (MJO) is a tropical wave that has lower and upper-level anomalies that produce enhanced convection. The convection formed by the MJO can provide enough low level vorticity that a TC can form, given that other necessary conditions are also favorable. Frank and Roundy (2006), showed that 25 percent of the TCs that form in the NA did so when the convective phase of a MJO was present.

3. North Atlantic Oscillation

The North Atlantic Oscillation (NAO) represents a variation in atmospheric mass between southern and northern dipoles centered near the Azores and Iceland. In the positive NAO phase, there is above (below) normal sea level pressure in the southern (northern) dipole; the opposite is true in the negative NAO phase. Frank and Young (2007) show that a positive NAO and a negative Southern Oscillation index (associated with EN) tends to lead to a drastic decrease in TC formations in the NA.

4. Atlantic Multi-decadal Oscillation

The Atlantic Multi-decadal Oscillation (AMO) is a multi-decadal variation in NA sea surface temperature (SST) and other atmospheric and oceanic variables. The warm (cool) phase of the AMO tends to coincide with an increase (decrease) in NA TC activity (Wikipedia 2009).

C. CLIMATE PREDICTION PROCESS

1. Definitions

a. Climatology

TC climatology provides a time averaged description of TC activity; for example, the frequency of tropical cyclone formation in a given region and period. Generally, the time average is constructed from 30 or more years of data to produce a long term mean (LTM). LTM descriptions of TC activity can be used to estimate future TC activity, and they can provide good descriptions of that

activity for relatively long periods and large regions. Thus, TC climatologies are commonly used as a standard against which to assess forecasts. However, LTM climatologies tend to do poorly for short periods and small regions, and they of course do poorly in describing variations from LTMs (e.g., interannual variations associated with ENLN).

b. Smart Climatology

We define smart climatology as state-of-the-science climatology that directly supports the Department of Defense (DoD). Smart climatology takes advantage of modern climate data sets, and modern climate analysis and forecasting methods, to better account for the full range of spatial and temporal variability in the climate systems. Smart climatology provides major improvements over traditional climatology, which is limited mainly to a LTM perspective based on observational data (as opposed to analysis or reanalysis data). U.S. military climatologies are almost exclusively traditional climatologies.

c. Tropical Cyclone

Tropical cyclone (TC) is the general term for a warm-core cyclone that forms over the tropical ocean (Glickman 2000). By international agreement, a TC is further broken down by maximum sustained winds: tropical depression (TD) less than 17 m/s, tropical storm (TS) 18-32 m/s, and hurricane (or typhoon or cyclone) 33 m/s or greater (Glickman 2000).

d. Intraseasonal Forecast

An intraseasonal forecast is a forecast with a lead time of approximately 14-70 days.

e. Large Scale Environmental Factors (LSEFs)

A large scale environmental factor (LSEF) is a climate system variable that has significant impacts on the formation of TCs (e.g., sea surface temperature (SST), low level relative vorticity, vertical wind shear, etc.).

2. Operational Climate Prediction and Long Range Forecasting

Figure 1 from Mundhenk (2009) outlines the processes of operational climate prediction and long range forecasting. For this study, we applied all but

the final steps in this process. These steps are described more fully in Chapter II and explained by example in the results of our study shown in Chapter III.

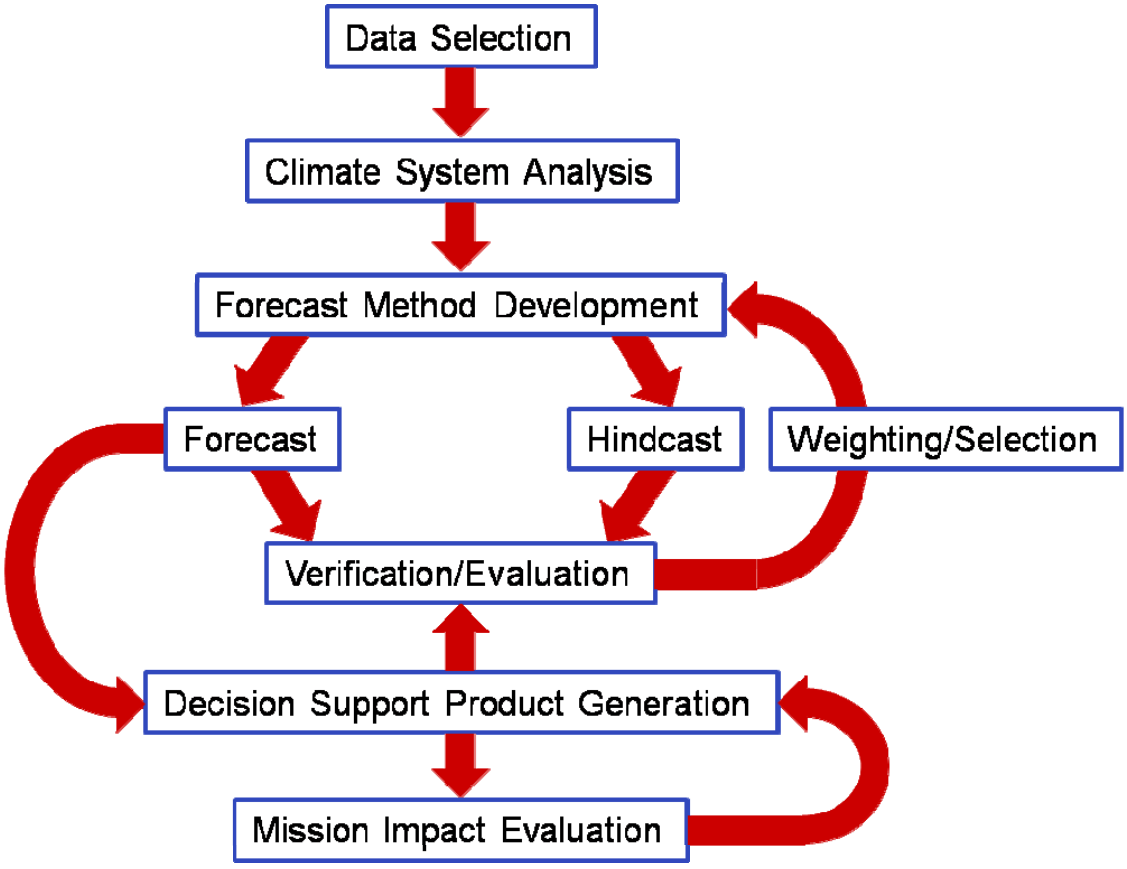

Figure 1. Outline of the process by which operational climate prediction and long range forecasting is done. From Mundhenk (2009).

3. Methods of Prediction

One of the most complex steps in the climate prediction and long range forecasting process (Figure 1) is step three, Forecast Method Development. This step involves deciding which predictive method to choose from—in particular, a statistical, dynamical, or a combined statistical-dynamical method.

a. Statistical

Most operational climate prediction centers (the National Weather Service's (NWS) Climate Prediction Center (CPC)) use statistical methods to forecast at intraseasonal to interannunal lead times. Statistical methods are

based on analyses of past states of the climate system that provide information on the probabilities of different states developing in the future.

b. Dynamical

Dynamical methods (e.g., methods involving the use of numerical versions of the dynamical equations for the atmosphere and ocean) tend to be relatively skillful for lead times out to about two weeks. However, the skill of dynamical methods tends to be lower than that of statistical methods for long lead times. Thus many dynamical methods are used for shorter lead times (e.g., less than one month) but are phased out in favor of statistical methods for longer lead times. However, the skill of dynamical methods at longer lead times has been increasing. One example of the application of dynamical methods for intraseasonal to seasonal forecasting is the National Centers for Environmental Prediction (NCEP) Climate Forecast System (CFS), a coupled atmosphere-ocean dynamical model system used by CPC. In 2005, the CFS developers received an award for excellent work. The occasion marked "the first time in history numerical seasonal predictions were on par with empirical methods" (van den Dool 2007).

c. Combined Statistical-Dynamical

Combinations of statistical and dynamical methods are also used, including weighted averaging of the outputs from statistical and dynamical forecasts. For example, some predictions of the number of TCs that will form in a basin during a TC season are based on both statistical and dynamical outputs. For example, the International Research Institute for Climate and Society (IRI) uses a combined method to experimentally predict the number of TCs that will form in the NA between August and October (Camargo and Barnston 2009).

For this study, we used a combined statistical-dynamical approach. We developed a statistical model that relates the LSEFs to the probability of TC formation. We then used intraseasonal predictions of the LSEFs from the CFS as inputs to our statistical model. The resulting output from the combined

statistical-dynamical model combination are probabilistic intraseasonal forecasts of TC formation. We chose the CFS because it is freely available to the public and it provides forecasts for lead times of several seasons. There are alternatives to the CFS, such as those from the European Centre for Medium-range Weather Forecasts (ECMWF). However, the output from these alternatives is not as readily available and/or as temporally extensive.

D. EXISTING PRODUCTS

1. Seasonal

Dr. William Gray at Colorado State University was the first to produce a seasonal TC forecast for the NA (Camargo 2006). These and other seasonal TC forecasts predict the aggregate number of TC formations in a given ocean basin for the overall TC season and the basin, without specifying the time or location of the formations within the season and basin.

The IRI experimental long range TC forecasts provide a probability of below-normal, normal, or above-normal TC formation probabilities for August through October in the NA basin. Figure 2 shows an example of an IRI TC forecast; IRI issues updates at the beginning of every month throughout the TC season. Such broad overview forecasts are useful but are limited in the value they provide to military planners and other planners because they lack specificity as to when and where individual TC formations are more and less likely.

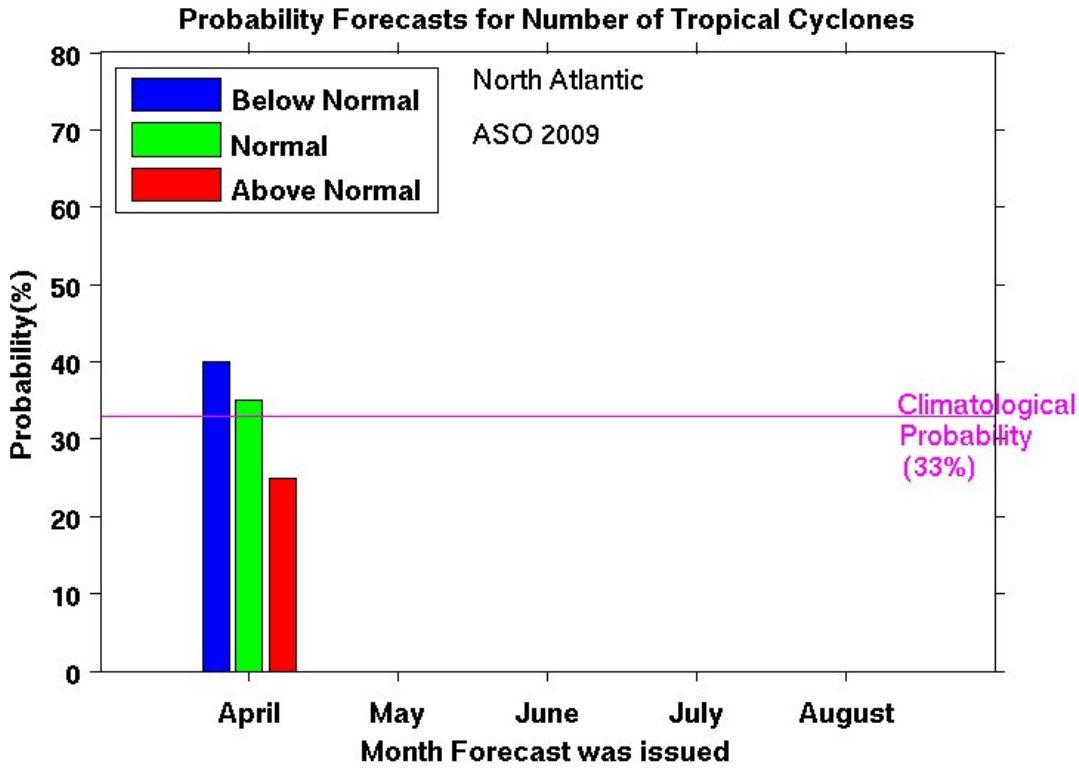

Figure 2. IRI probability forecast for the number of TCs in the NA during August-October 2009, issued by IRI on 1 April 2009 (IRI 2009).

Other prediction centers that currently produce a seasonal forecast include: Colorado State University, IRI, European Centre, City University of Hong Kong, NOAA, and Institute of Meteorology of Cuba.

In this study, we have developed and tested a statistical-dynamical approach to intraseasonal forecasting of the probabilities of formations for specific dates (individual weeks) and locations (individual 2.5 x 2.5 degree regions).

2. Intraseasonal

Intraseasonal forecasts provide information on TC activity for intraseasonal periods (e.g., one month within a TC season). Intraseasonal forecasts also tend to be relatively specific about the location within a basin where TC activity is likely. This greater temporal and spatial specificity means that intraseasonal forecasts, if they are skillful, have the potential to be much

more useful to planners than seasonal forecasts. Some of the long range prediction centers mentioned in the seasonal section are also developing intraseasonal forecasts.

Frank and Roundy (2006) used the Madden-Julian oscillation (MJO) and other tropical waves to create a 30-day outlook of daily probabilities for TC formation around the globe. Roundy makes these experimental forecasts freely available through his homepage at the State University of New York at Albany (Albany 2009). Leroy and Wheeler (2009) use a similar approach for southern hemisphere TCs, using five predictors: the climatology cycle, two associated with the MJO, and two associated with SST. Unfortunately, these forecasts are not freely available to the public.

Though these statistical methods show great promise, Camargo (2006) states that "while there is much room for improvement in the skill and application of empirical/statistical methods of intra-seasonal TC prediction, the greatest hope for improvement lies with dynamical/numerical models." The ECMWF produces such a dynamical forecast for TC formation via their Ensemble Prediction System (EPS) for the seven ocean basins; however, it is not freely available to the public.

The CPC issues operational intraseasonal TC forecasts that are available free online. Figure 3 depicts an example a two-week TC formation outlook that is part of the CPC Global Tropics Benefits/Hazards Assessment. This product has a graphical depiction of the hazards in the tropics and text that explains the hazards. The text that explains the red highlighted area labeled "2" in the middle of the NA states (CPC 2007):

> The potential for tropical cyclone development across the deep tropical Atlantic Ocean. It is anticipated that a northward displaced and enhanced African Easterly Jet will continue to aid in the development of Robust African easterly waves and with areas of above average SSTs and weak vertical wind shear the chances of tropical development are increased. Confidence: Moderate.

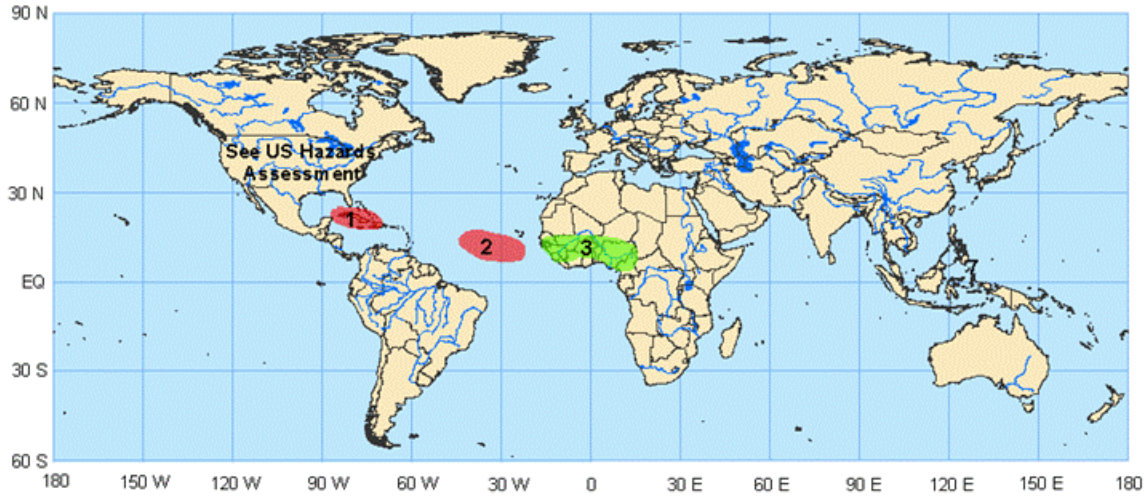

Figure 3. CPC Global Tropics Benefits/Hazards Assessment for 21-27 August 2007, issued by CPC/NCEP on 13 August 2007 (CPC 2007).

This CPC product is generated using a subjective blending of forecast tools, but CPC plans to make this product more objective (Gottschalck et al. 2008). In this study, we have explored one method for making such predictions more objective and have discussed with CPC the potential for applying this method to improve the CPC Global Tropics Benefits/Hazards Assessment.

3. DoD Products

The DoD currently does not produce any seasonal or intraseasonal TC formation forecast products for any ocean basin. The Joint Typhoon Warning Center (JTWC) and the 14th Weather Squadron (14WS) provide very limited climatology products, but no explicit seasonal or intraseasonal TC forecasts are available.

E. RESEARCH MOTIVATION AND SCOPE

1. Closely Related Prior Work

Meyer (2006) took a statistical approach to studying TC formation regions in the WNP. Though his research only provided zero lead hindcasts using the National Centers for Environmental Prediction (NCEP) reanalysis data, Meyer

showed that if the LSEFs can be predicted at long leads, we should be able to use logistic regression to calculate long range forecasts of the probabilities for TC formation.

Mundhenk (2009) followed Meyer's work and took a statistical-dynamical approach to predicting TC formation regions in the WNP. Mundhenk produced a regression model that was trained on NCEP reanalysis data. However, he then forced that model with operational Climate Forecast System (CFS) fields and produced non-zero lead TC formation probabilities for the WNP. With limited verification, these non-zero lead forecasts appeared to provide skill and value beyond that of standard climatology.

2. Research Questions

This thesis will follow the path of Mundhenk (2009) and address the same questions for the NA that he answered for the WNP:

1) Can favorable regions for TC formation be predicted at intraseasonal lead times in the NA using the CFS?

2) Do these predictions have more skill than standard climatology?

3. Thesis Outline

Chapter II discusses the region we chose to investigate, the timeframe we used, and the data sets and methods used in creating our regression model. The various LSEFs that were investigated are discussed as well. This chapter also summarizes the various methods we used to verify our hindcasts and forecasts.

Chapter III provides details of the regression model and the verification of our model. We then show examples comparing our TC formation forecasts to that of standard climatology. Finally, we provide examples of non-zero lead forecasts from the CFS.

In Chapter IV, we provide a summary of our work, our conclusions, and our recommendations for future endeavors in intraseasonal TC formation forecasting.

II. DATA AND METHODS

A. STUDY PERIOD AND REGION

We chose the NA as our study region because of the importance of NA TCs for the United States and military operations in the region. Figure 4 depicts the NA region we investigated during this study, 15° W-100° W and 7.5° N to 37.5° N. The years we focused on are 1970-2007. From the National Oceanic and Atmospheric Administration (NOAA) best track data (NOAA 2007), there are approximately 11 TC formations in the NA per year. Note from Figure 4, that our NA region only excludes one TC that formed during 1970-2007. Later in this chapter, we cover in more detail why we excluded 0°-7.5° N from our data set.

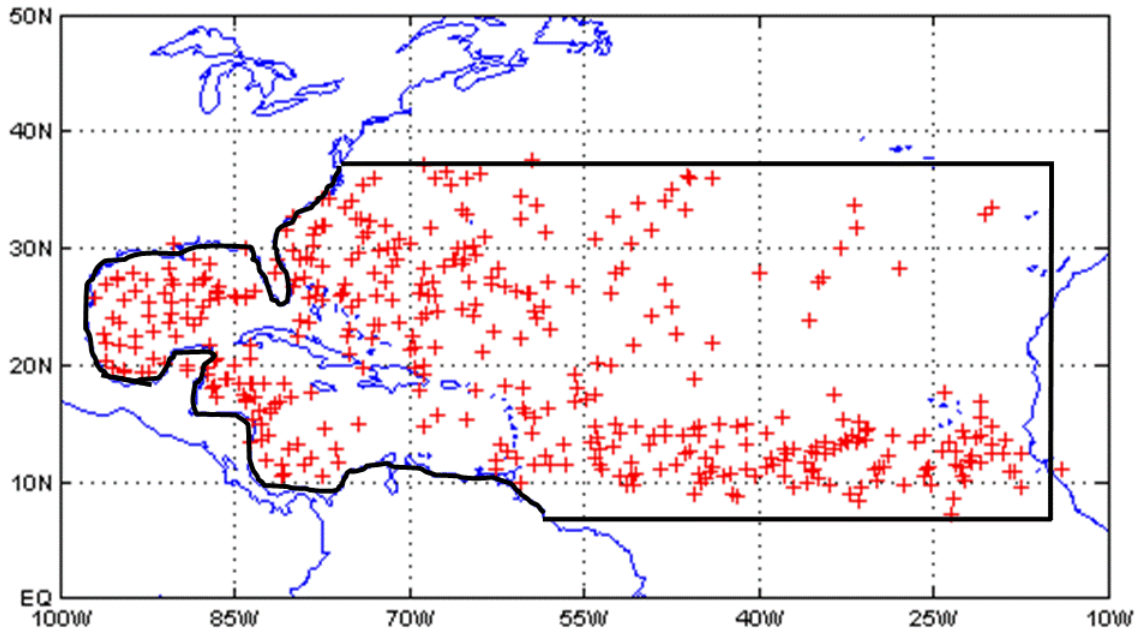

Figure 4. The NA study region (outlined by the black box) and TC formation points during 1970-2007 (red crosses), constructed from NOAA best track data.

B. DATA SOURCES

1. NOAA Best Track

NOAA's Atlantic Oceanographic and Meteorological Laboratory maintains a TC best track data set called HURDAT (NOAA 2007). Figure 4 shows the TC initial locations of NA TCs during 1970-2007 as identified by HURDAT. Note the large number of formations in main development region for NA TCs, the tropical Atlantic at 10^{o}N-20^{o}N and between northern South America and western North Africa. Unlike the JTWC TC best track archive, HURDAT only provides archives of storms that became a TS or greater. Therefore, if a TC only reached TD intensity, it would not be captured in this data set. Further, HURDAT only provides TC information starting from the time and location at which the TC reached TD intensity. This is a major difference between Mundhenk (2009) and our research in the NA. The JTWC best track data used by Mundhenk (2009) trace individual TCs back to the time and location at which the initial convection could be identified. The JTWC data also includes storms that only reached TD intensity. Thus, for example, the JTWC data has formation points with 2 m/s as the maximum sustained winds, while in the NA, the initial information for the TCs goes no lower than 13m/s maximum sustained winds.

Figure 5 shows the occurrence by month of NA TCs during 1970-2007, with a peak during the months of July-October (JASO). For our model development, we extended beyond this peak period a little and used HURDAT from June-November. We chose to do so to include as many TCs as possible ion our model development, while also limiting the development to the period with the greatest TC activity. We wanted to provide as many storms as possible to the logistic regression model to ensure optimal model performance.

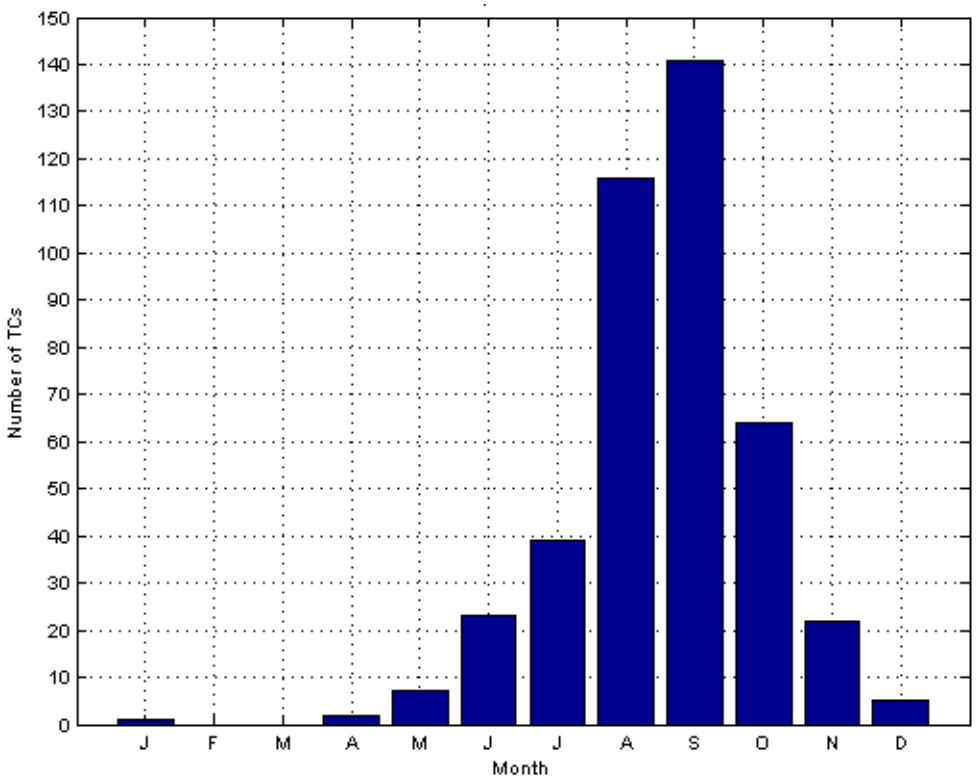

Figure 5. Number of NA TC formations versus month of the year, constructed with NOAA best track data from years 1970-2007.

2. NCEP Reanalysis

We chose the NCEP/Department of Energy Atmospheric Model Intercomparison Project-II as the reanalysis data set (hereafter referred to as R2) on which to train our regression model (Kanamitsu et al. 2002). The R2 data set covers 1979-present at a T62L28 resolution. The R2 data set we used has a 2.5° x 2.5° horizontal resolution and daily temporal resolution.

3. NOAA OISST

We used the National Oceanic and Atmospheric Administration (NOAA) optimum interpolation (OI) SST analysis version 2 (Reynolds et al. 2002). NOAA uses both in situ and satellite observations to produce a 1° spatial resolution and a weekly temporal resolution covering 1982-present. To match the R2 and SST

data sets to match, we extrapolated the 1° spatial resolution SST data set to 2.5° and interpolated the weekly temporal resolution SST to daily.

4. NCEP CFS

We used the CFS as the source of long range forecasts of the LSEFs to force our regression model when generating non-zero lead forecasts. The CFS is a fully coupled ocean-land-atmosphere dynamical model used to forecast at seasonal lead times (Saha et al. 2006). The CFS became operational at NCEP in late 2004 and provides four daily forecasts that have nine-month lead times (Saha 2008).

The atmospheric component of the CFS uses the coarser resolution of the Global Forecast System (GFS), so the CFS has approximately 1.8° resolution. We extrapolated the CFS to 2.5° spatial resolution to fit our R2 resolution. The ocean component of CFS uses the Geophysical Fluid Dynamics Laboratory (GFDL) Modular Ocean Model version 3 (MOM3). Four CFS runs are executed daily, with integrations out to nine months. We used all four CFS runs to create ensembles to best capture the LSEFs. The CFS runs, like other dynamical long range forecast models, tends to converge toward climatology. To remedy this situation, NCEP provides bias correction files that we employed to remove this systematic error.

The CFS does not provide the full suite of variables offered by R2, such as vorticity and divergence. The CFS variables that we used directly are SST and winds at 850 and 200 mb. However, we used these CFS winds to calculate vorticity and divergence at 850 and 200 mb, as done by Mundhenk (2009).

C. VARIABLES OF INTEREST

1. Classical LSEFs

Though Gray (1968, 1975, 1979) identified six large-scale environmental conditions or factors needed for TC development that he called genesis parameters. There are many lists of LSEFs, but all lists are slight variations of

Gray's original. In addition to the presence of favorable LSEFs, TC formation probably also requires, in general, one of several possible triggering factors—for example, a pre-existing disturbance—in order for TC formation to occur (Gray 1968; Emanuel 1989; Zehr 1992).

a. Sea Surface Temperatures

Meteorologists have known the relationship between high SSTs and TC formation for about 60 years. Palmen (1948) found that TCs rarely form when SSTs were below 26.5 °C. Our research agrees with his findings, with only 21 out of 273 NA TCs that formed during 1982-2006 having done with SSTs below 26.5 °C.

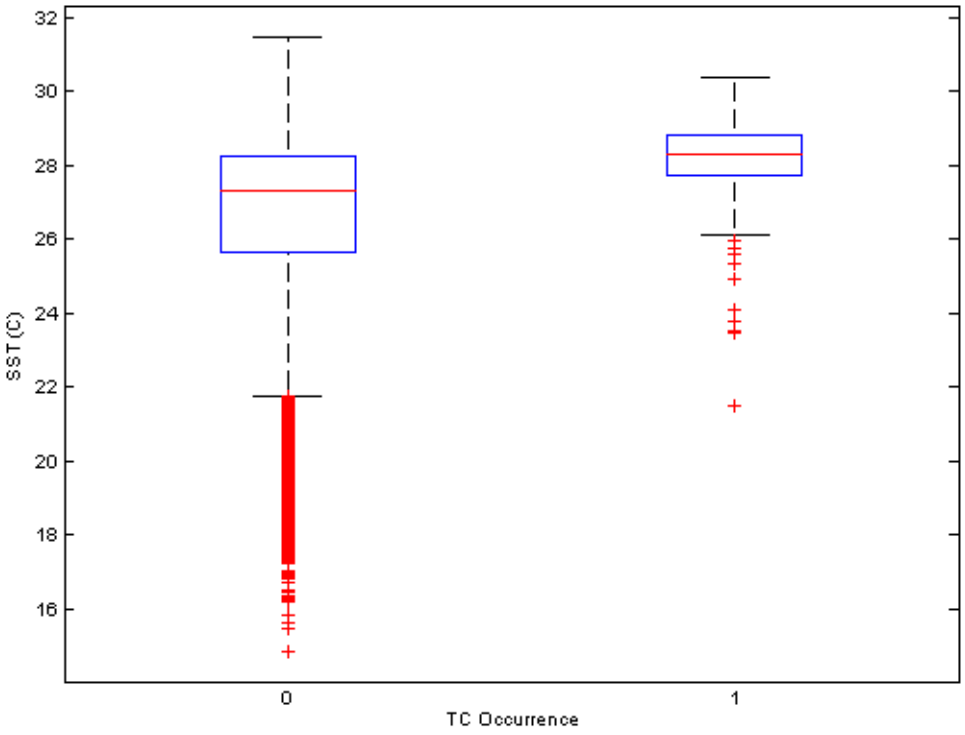

Figure 6. Box plots of SST (in °C) grouped by whether a TC formed in a given day-grid ("0" indicates no TC formed, and "1" indicated a TC formed). The blue box encloses 50% of the SST data points, the whiskers (black dashed lines) encompass ~99% of the data points. The red "+" highlight ~1% of the data points that are outliers. Produced using NOAA OISST data and TC occurrences from the HURDAT for January-December of 1982-2006.

Figure 6 depicts the box plots that separate grid point values of SST on individual days when a TC did not form (“0”, on the left) and on days when a TC did form (“1”, on the right). Less than 8 percent of the TCs that formed in the NA from 1982 to 2006 formed with SSTs below 26.5 °C. Figure 6 also indicates that the SSTs associated with TC formations are relatively distinct from those associated with non-formation times and locations.

b. Humidity

The importance of mid-level humidity in TC formation has been well documented. Recently, Dunkerton et al. (2009) presented the marsupial metaphor to describe a critical layer gyre that contains mid-level moisture that favors deep convection and TC formation.

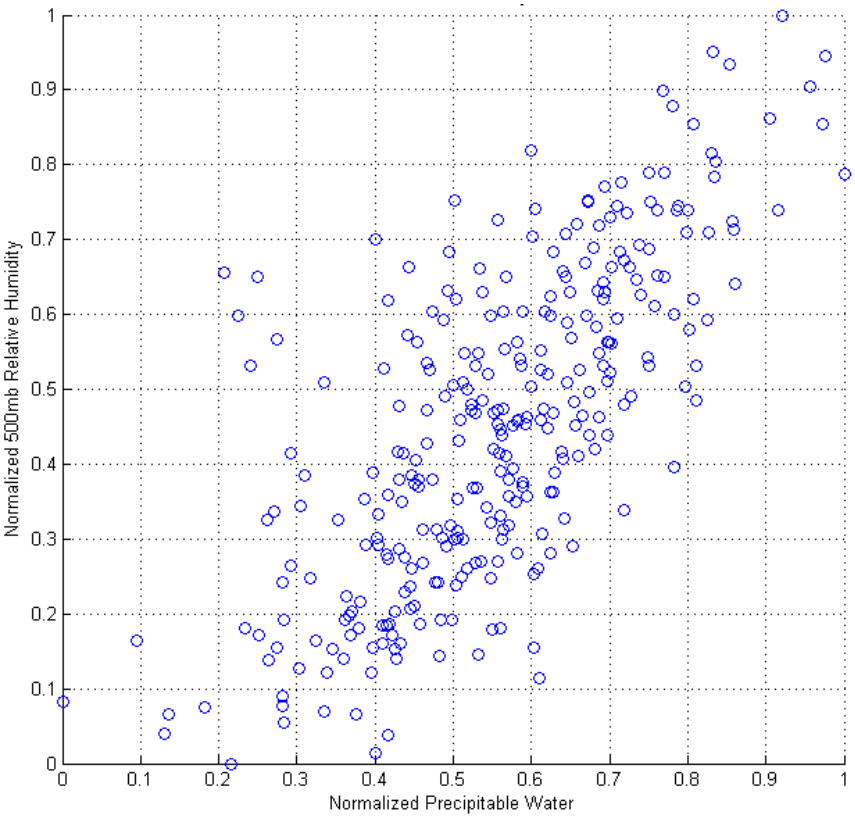

Figure 7. Normalized scatter plot of North Atlantic January-December precipitable water vs. 500 mb relative humidity. Note the strong relationship between the two variables. Constructed from R2 data from 1982-2007 for dates and locations at which TCs occurred.

The CFS does not provide relative or specific humidity as output variables, so we chose to use precipitable water as a replacement for humidity. Figure 7 shows that there is a strong positive correlation (0.72) between R2 500 mb relative humidity and precipitable water at the times and locations at which NA TCs formed. Thus, we concluded that precipitable water is an adequate substitute for mid-level relative humidity.

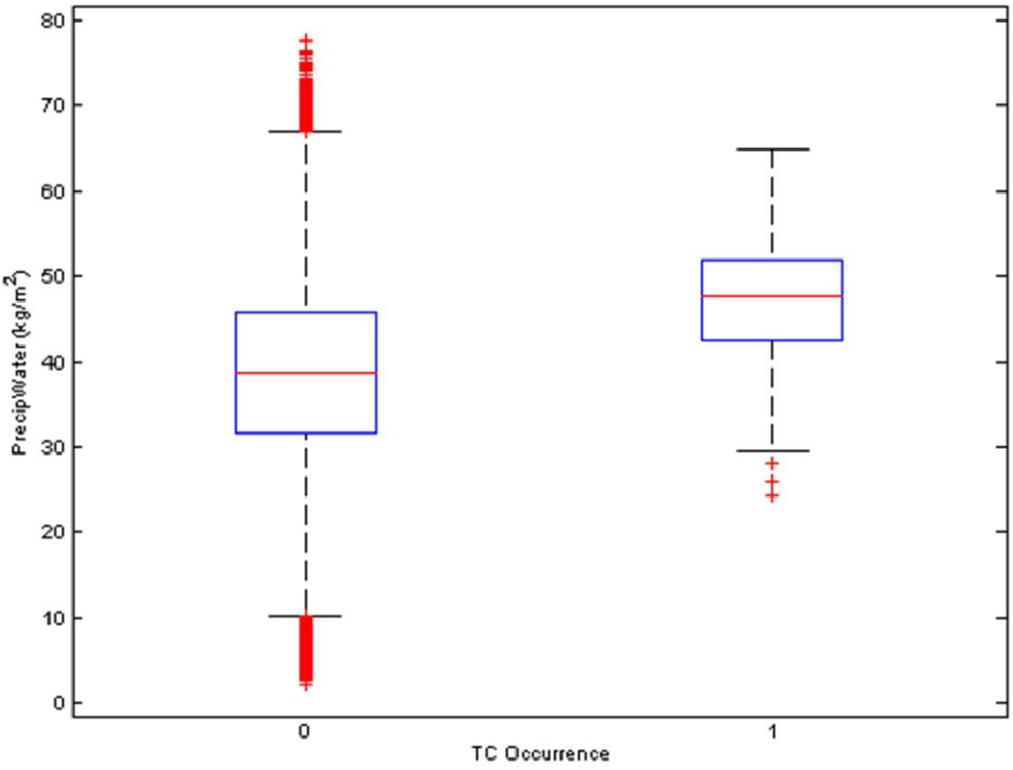

Figure 8. Box plots of precipitable water (kg/m^2) grouped by whether a TC formed in a given day-grid ("0" indicates no TC formed, and "1" indicates a TC formed). The blue box encloses 50% of the precipitable water data points, the whiskers (black dashed lines) encompass ~99% of the data points. The red "+" highlight ~1% of the data points that are outliers. Produced using R2 data and TC occurrences from the HURDAT for January-December of 1982-2006.

Figure 8 depicts the box plots for precipitable water with "0" indicated the non-TC information (NTCI) and "1" indicating the TC formation data. Figure 8 also indicates that the precipitable water values associated with TC formations are relatively distinct from those associated with non-formation times

and locations. However, the corresponding NTCI and TC box plots for 500 mb relative humidity (not shown) are nearly identical. This indicates that precipitable water may be a better variable than relative humidity for our logistic regression model.

c. Wind Shear

Many past studies have shown that the greater the vertical wind shear, the less likely it is for TC formation (Gray 1968; Emanuel 1989; Zehr 1992). As in most prior studies, we defined vertical wind shear as the 200 mb vector wind minus the 850 mb vector wind. This result gives us a magnitude and direction; however, in this study we only used the magnitude of the vertical wind shear.

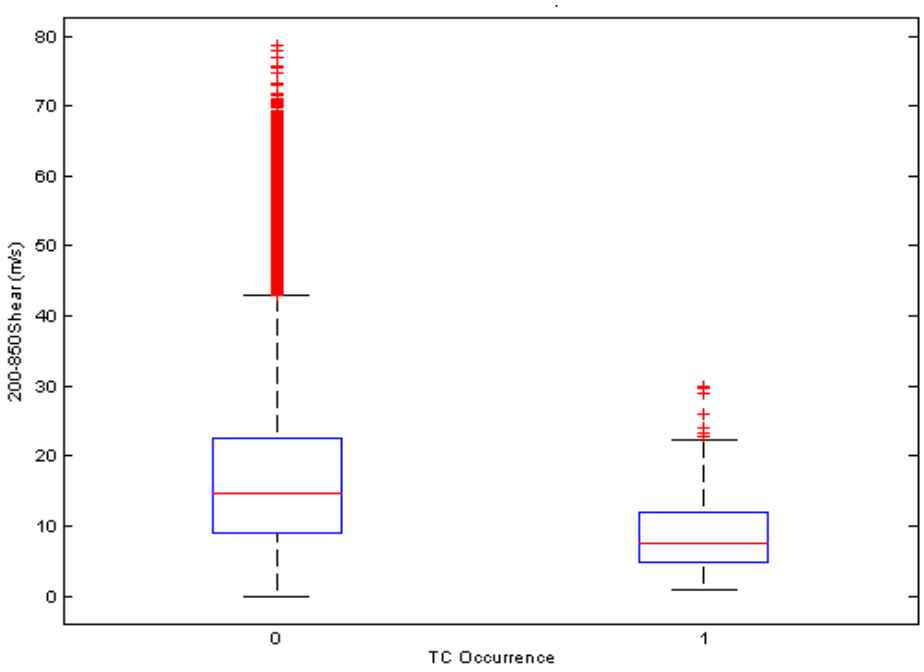

Figure 9. Box plots of 200-850mb wind shear (in m/s) grouped by whether a TC formed in a given day-grid ("0" indicates no TC formed, and "1" indicated a TC formed). The blue box encloses 50% of the wind shear data points, the whiskers (black dashed lines) encompass ~99% of the data points. The red "+" highlight ~1% of the data points that are outliers. Produced using R2 data and TC occurrences from the HURDAT for January-December of 1982-2006.

Figure 9 clearly highlights that low wind shear is associated with TC formation in the NA, while generally higher wind shear is present when there are no TC formations. Seventy-five percent of the TCs form with shear below 12 m/s and 99 percent form with a wind shear less than 22 m/s.

d. Upward Vertical Motion

Like 500 mb relative humidity, 200 mb omega is not available in the CFS package, so we decided to use 200 mb divergence as an alternative to represent upward vertical motion. Since 200 mb divergence is not available through CFS either, we calculated it via second order centered finite differencing of the 200 mb wind. The correlation between R2 200 mb divergence and 500 mb omega is -0.77 (see Figure 10). The negative correlation indicates that when 500 mb omega is negative (indicating upward motion), 200 mb divergence is positive (indicating upper level divergence consistent with mid-level upward motion), and vice versa. Figure 11 depicts the box plot for 200 mb divergence. Of the 303 TCs that formed from 1982 to 2007, 91 percent did so with upper-level divergence. Thus, upper-level divergence appears to be good candidate for our logistic model.

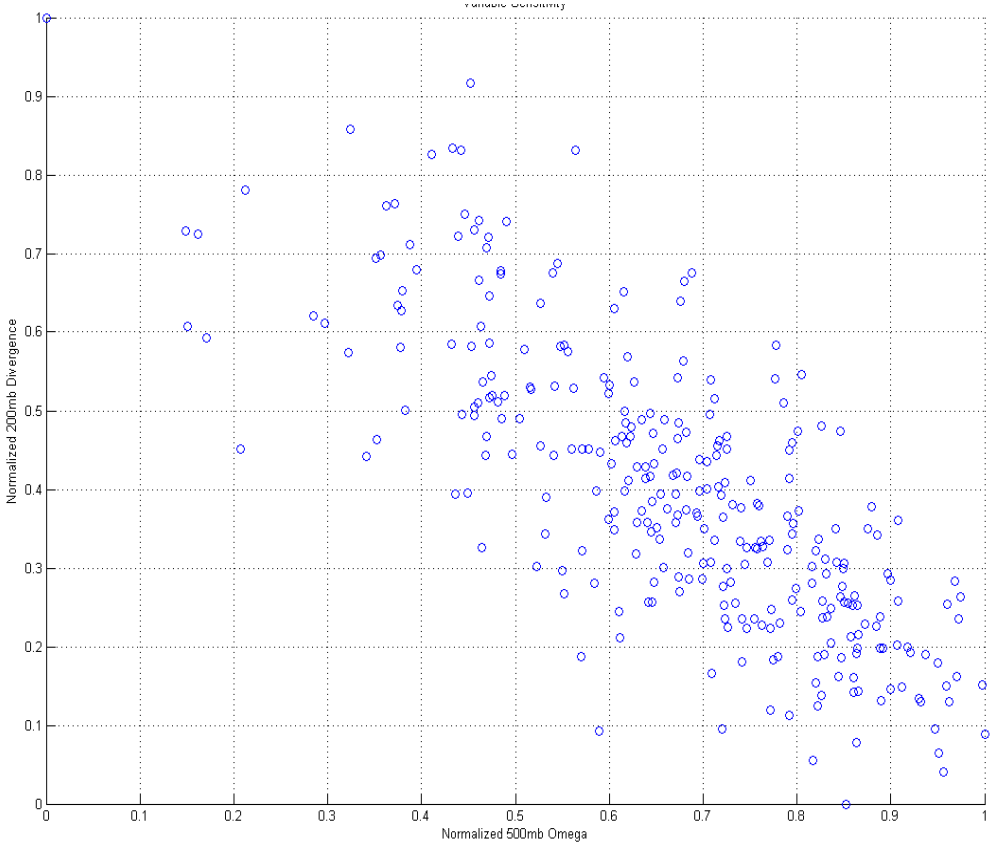

Figure 10. Normalized scatter plot of January-December 200 mb divergence vs. 500 mb omega. Note the strong negative correlation between the two variables. Constructed from R2 data from 1982-2007 for times and locations at which TCs occurred.

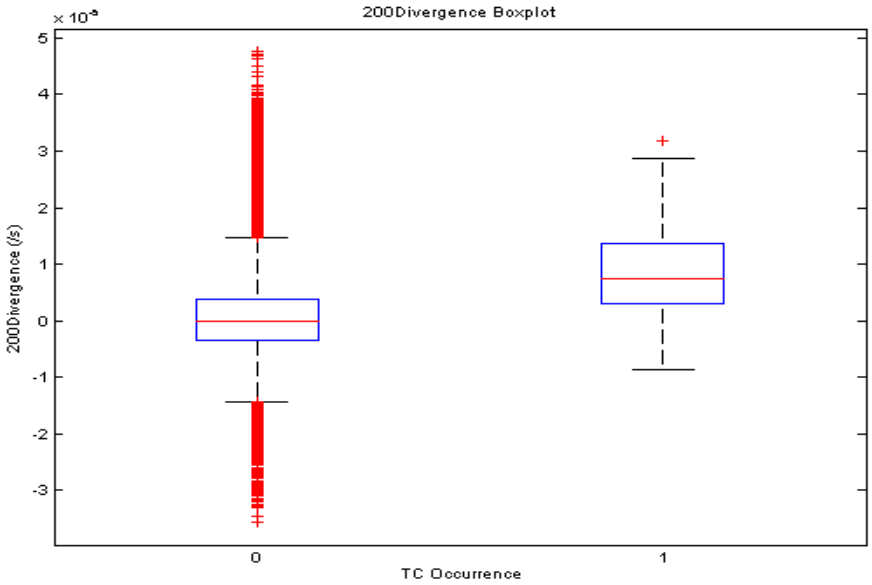

Figure 11. Box plots of 200 mb divergence (in /s) grouped by whether a TC formed in a given day-grid. The blue box encloses 50% of the divergence data points, the whiskers (black dashed lines) encompass ~99% of the data points. The red "+" highlight ~1% of the data points that are outliers. Produced using R2 data and TC occurrences from the HURDAT for January-December of 1982-2006.

e. Low-Level Vorticity

The occurrence of lower-level positive relative vorticity is important for TC formation. The box plots in Figure 12 indicate that only seven NA TCs during 1982-2006 formed with negative relative vorticity at 850 mb. Thus, we selected low-level relative vorticity as a potential LSEF for our logistic regression model.

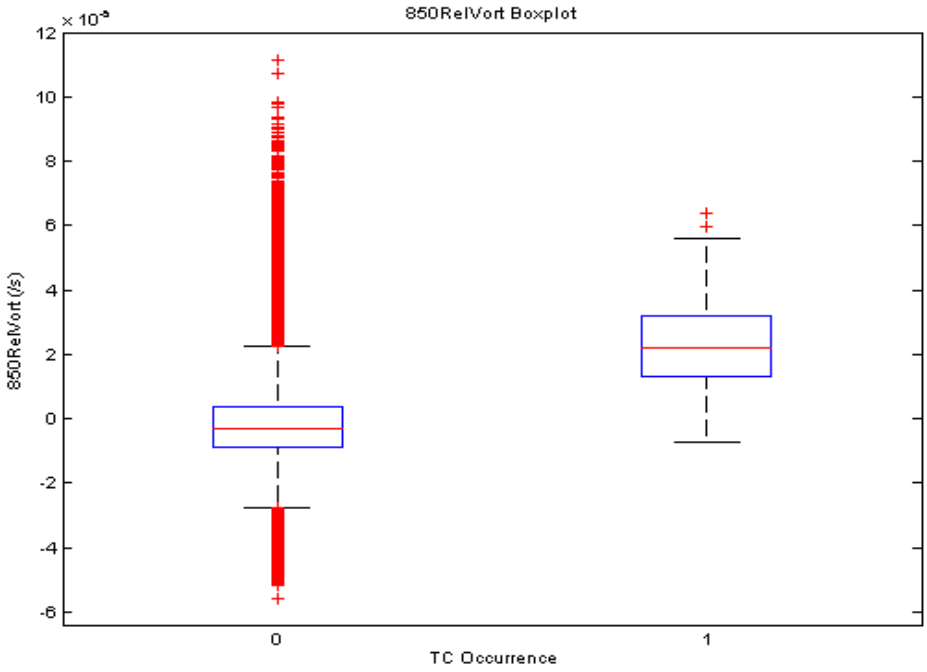

Figure 12. Box plots of 850 mb relative vorticity (in /s) grouped by whether a TC formed in a given day-grid. The blue box encloses 50% of the vorticity data points, the whiskers (black dashed lines) encompass ~99% of the data points. The red "+" highlight ~1% of the data points that are outliers. Produced using R2 data and TC occurrences from the HURDAT for January-December of 1982-2006.

We also investigated using planetary vorticity and absolute vorticity as LSEFs. The occurrence of only one TC formation south of 7.5° N indicates that planetary vorticity has a positive relationship with TC formation. Thus, we included a Coriolis term in the model to account for this dependence on planetary vorticity (see Chapter III). We chose not to use absolute vorticity as an LSEF, because the model performed better when using separate relative vorticity and Coriolis terms than when using absolute vorticity alone.

2. Non-Classical LSEFs

To reduce the risk of excluding important LSEFs, we investigated a number of addition variables available in R2 for use as LSEFs in the regression model, including:

1) Mean sea level pressure

2-5) 850 mb: relative humidity, divergence, omega, and temperature

6-9) 500 mb: relative vorticity, absolute vorticity, divergence and temperature

10-15) 200 mb: relative humidity, relative vorticity, absolute vorticity, divergence, omega, and temperature

16-18) Thickness: 200-850 mb, 500-700 mb, and 500-850 mb

Based on verification and other analyses of the outputs from test models that using the full range of LSEFs (see Section D, Chapter II), we rejected variables 1-18 (above) for use in our logistic regression model. The final set of LSEFs that we used (see Section D, Chapter II) is very similar to the set specified by Gray (1968, 1975, 1979).

D. PROBABILISTIC EQUATION DEVELOPMENT

1. Logistic Regression

We used logistic regression to create our TC formation probability forecast using the LSEFs as our independent variables. For exact details on logistic regression the reader is referred to Wilks (2006) or a similar college level statistics book. It is important to note that our LSEFs are not completely independent of each other. For example, a region of positive low-level vorticity and high SSTs will also have high relative humidity. Therefore, positive low-level vorticity and high relative humidity are positively correlated. Ideally, this sort of correlation between LSEFs would not exist, and its existence makes model building, and interpretation of the results, more challenging.

2. Model Training

We wanted to use the best data available to train our regression model, so we chose data only from the satellite era (approximately 1970-present). As stated before, we chose R2 and OISST data to train our model; therefore, our

training data set was limited to 1982-2008. Ultimately, we chose to include only LSEF data from the peak formation period, June through November, to minimize data dilution (Eckel 2008).

As discovered by Mundhenk (2009) in the WNP, our model has a tendency to underpredict. Underprediction occurs when the forecast probability is below the observed frequency. Thus, our model tends to forecast lower TC formation probabilities than the actual observed TC formation probabilities. The reason for this shortcoming of the model is that the days and locations immediately surrounding the time and place at which a TC forms tend to have LSEF values that are favorable for formation. However, TCs tend to form in relative temporal and spatial isolation from each other (with a small number of exceptions). Thus, the model assigns a lower probability of formation to those conditions based on the lack of formation during the surrounding times and locations. The net result is that the regression model tends to predict lower formation probabilities than observed.

To remedy this underprediction, we chose to exclude 60 percent of the non-TC information (NTCI) from the R2 and HURDAT data sets. When 100 percent of the NTCI were used, the model vastly under-predicted TC formation probabilities. We also decided not to use data below 7.5° N because there has only been one NA TC since 1970 that formed south of 7.5° N (see Figure 4).

3. Model Selection

We ran our regression model numerous times with different LSEF variables, amounts of NTCI, and start and end dates. First, we ran each LSEF separately to find which LSEFs had the strongest relationships with TC formation. We then ran all possible combinations of these LSEFs to ensure we had the best combination of variables possible based on the results of various scoring methods. Second, we tried 40, 50, 60, 80, and 100 percent NTCI to address the under-prediction problem mentioned above. Third, we ran with various start and end dates for the LSEF and TC data to ensure we were not

using too much data from months in which TC formation is rare. This was a delicate balance because if we chose just JASO, we would have excluded too many TC formation points, which would have reduced the skill of our regression model. We settled on using data from June-November to develop the regression model.

As statistical forecasting is recently new, especially for an event as rare as a TC, finding a suitable set of methods to score the model results was not an easy task. As discussed by Mundhenk (2009), we selected the following as the tools with which to test our model.

a. Akaike Information Criterion

Akaike information criterion (AIC) is a measure of the goodness-of-fit of a statistical model with a penalty for added independent variables to counter tendencies toward over fitting. Low values of AIC indicate the preferred model; that is, the model with the fewest independent variables that still provides a good fit to the data. We direct the reader to Burnham and Anderson (2002) for a more detailed explanation of AIC.

b. Deviance

We used residual deviance to compare models developed from different LSEFs, NTCI, and start and end dates. Deviance determines how well the given equation accounts for variability: the lower the residual deviance of a model, the better the goodness-of-fit of that model.

c. Stability

To ensure a stable model, we used the jackknife approach to create our model. We ran the regression model from 1982-2006, first excluding the year 1982, second excluding the year 1983, and so on. We compared each of these logistic regression equations to ensure stable coefficients (indicated by coefficient changes that are small from one run to the next). We then took, for

each LSEF, the average of all the coefficients from the different runs, to come up with the coefficients for our final linear regression model equation.

d. Physical Plausibility

One might expect that a regression model would return an equation that is physically plausible, but this was not always the case. For example, we know that positive low-level relative vorticity is positively correlated with TC formation, so a model that returned results with a negative coefficient for low-level relative vorticity would be identified as physically implausible. This sort of physically implausible coefficient and implied relationship between an LSEF and TC formation probability arose in some cases when we included LSEFs that are closely correlated with each other. For example, when we included variables representing low-level relative vorticity, SST, vertical velocity, and relative humidity, the regression process assigned a negative coefficient to relative humidity. This was because of the positive correlations between relative humidity and the other LSEFs in the same model (SST, low level relative humidity, vertical velocity). As stated above, the LSEFs are not independent; therefore, we chose to strike a delicate balance between goodness-of-fit and model complexity, as we felt physical plausibility was an important, desirable model attribute.

4. Model Verification

Prior to our research, no one had published, to our knowledge, a complete set of methods for verifying probabilistic forecasts of individual TC formations. Thus, we developed a set of several verification metrics applied in unison to verify our model. The metrics we used are: hits, misses, Brier score (BS) Brier skill score (BSS), relative operating characteristic (ROC), and reliability.

We also created anomaly probabilities with both our hindcasts and forecasts probabilities. The anomaly probability is our forecasted probability minus the corresponding climatological probability. The resulting forecast

probability anomaly provides a clear depiction of how our forecasts differ from normal probabilities, which can be very useful to planners who are familiar with normal probabilities and risks.

E. SUMMARY OF PREDICTION METHOD

Figure 13 (adapted from Mundhenk 2009) illustrates the process we used in this study. As Mundhenk (2009) explains, "this process is a combined statistical-dynamical one, wherein one uses a numerical model to force a statistical model to generate ensemble based, probabilistic, intraseasonal predictions of TC formations."

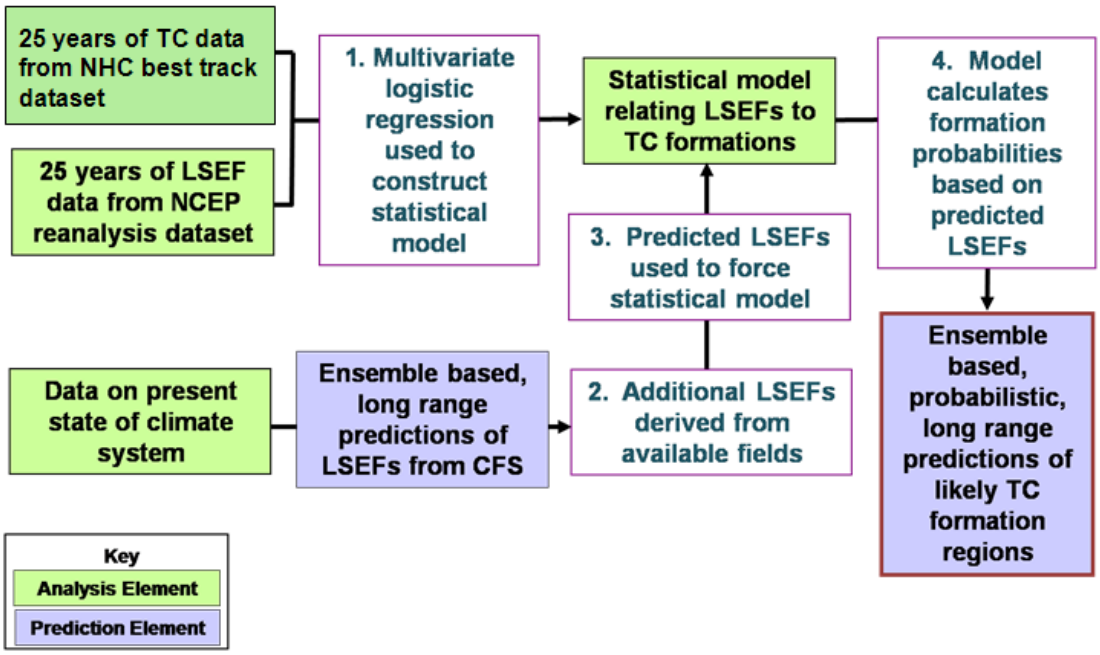

Figure 13. Depiction of the process for generating intraseasonal predictions of tropical cyclogenesis (adapted from Mundhenk 2009).

THIS PAGE INTENTIONALLY LEFT BLANK

III. RESULTS

A. REGRESSION MODEL

We employed logistic regression to construct an equation for the probability of TC formation in a given 2.5 ^{o} x 2.5 ^{o} block on a given day. Logistic regression finds best estimates of the intercept b_0 and the coefficients b_k for each LSEF (x_k). This leads to the probability of TC formation (p_F) at a given day grid point:

$$p_F = \frac{e^{(b_0 + b_1 x_1 + ... + b_6 x_6)}}{1 + e^{(b_0 + b_1 x_1 + ... + b_6 x_6)}}$$

His equation is the regression model developed and tested in this study. Table 1 lists the LSEFs and their coefficients of the optimal version of this equation. The optimal model was selected from all the models we developed and tested by goodness of fit and the other considerations described in Sections III.A.1 and III.A.2. The LSEFs in the optimal version of the regression equation are, in order of their significance as determined by a Chi-squared test: 850 mb relative vorticity, 850 mb relative vorticity squared (hereafter, RV2), SST, wind shear, 200 mb divergence, and a term representing Coriolis effects. We tested numerous other models, but this model provided the best fit between our LSEF data and TC formation data. The negative sign for the RV2 and wind shear coefficients indicates that when wind shear and RV2 increase, the probability of TC formation goes down. Conversely, the positive coefficients for 850 mb relative vorticity, SST, 200 mb divergence, and the Coriolis term indicate that when these variables increase, the probability of TC formation goes up. Therefore, the model summarized in Table 1 is physical plausible in terms of the coefficient signs.

Variable		Regression Coefficient		Significance Rank	Standard Error	t Value
-	(Intercept)	b_0	-21.4805624	-	1.441591	-15.10
x_1	850 mb Rel. Vort	b_1	239718.544	1	14316.48	16.81
x_2	850 mb Rel. Vort^2	b_2	-2897314840	2	257575600	-11.25
x_3	SST	b_3	0.459047508	3	0.04858943	9.64
x_4	Wind Shear	b_4	-0.09942719	4	0.01095125	-8.99
x_5	200 mb Divergence	b_5	54503.2704	5	8348.18	6.38
x_6	Coriolis	b_6	10576.12604	6	3493.039	3.12

Table 1. LSEF coefficients and related descriptive statistics for the optimal regression model developed and tested in this study. The model was developed using NA LSEF and TC data from June-November of 1982-2006, and included data from 40 percent of the NTCI time-location blocks.

For comparison, Table 2, from Mundhenk (2009), summarizes the regression model he developed and tested for long range forecasting of TC formations in the WNP. The similarities between the two models are striking, with both the LSEF variables and their significance rankings being the same for the NA and WNP. Gray (1968, 1975, 1979) implied that the genesis parameters applied in all the tropical basins, and the NA and WNP models seem to confirm his assertion. As noted in Section II.B.1, the data sets for the WNP and the NA are vastly different. The WNP had formation points when there was just convection present, while the NA data set had formation points only at TD strength. These differences might have led one to expect different regression models for the NA and WNP. Moreover, despite the similarities, there are some notable differences; for example, the differences in the magnitude of the VR2 term. The VR2 term is included in the model to reduce storm chasing, which is a tendency for the model to provide high probabilities at the time and location of a TC but well after the TC has formed. Unlike the WNP, the NA had a severe problem with storm chasing, which explains the difference in the RV2 magnitudes for the NA and WNP. Also, the Coriolis term is more important in the WNP than it is in the NA. This is partially due to the tendency for more low latitude formations in the WNP than in the NA (during 1970-2006, only one TC formed below 7.5° N in the NA, while many storms form below that latitude in the WNP).

Variable		*Regression Coefficient*		*Significance Rank*	*Standard Error*	*t Value*
-	(Intercept)	b_0	-27.41179	-	1.81639	-15.09
x_1	850mb Rel. Vorticity	b_1	167645.1	1	7074.82	23.69
x_2	850mb Rel. Vorticity^2	b_2	-1679802094.0	2	112033900	-14.99
x_3	SST	b_3	0.6567593	3	0.06061	10.83
x_4	Vertical Wind Shear	b_4	-0.05990173	4	0.00687	-8.71
x_5	Coriolis Parameter	b_5	15861.34	5	2646.58	5.99
x_6	200 mb Divergence	b_6	24729.49	6	6152.83	4.01

Table 2. LSEF coefficients and related descriptive statistics for the optimal regression model developed and tested for WNP TCs by Mundhenk (2009). The model was developed using WNP LSEF and TC data from June-November of 1982-2006, and included data from 40 percent of the NTCI time-location blocks.

As in the WNP, we had to include two adjustments to our model to focus the model on formation days rather than on days in which mature TCs occurred (Mundhenk 2009). This is important because the LSEFs present on the day of formation are very similar to those after the day of formation. To remedy this we first included a mean sea level pressure (MSLP) filter to eliminate NTCI for which MSLP was below 998 mb. Of the 273 TCs that formed during 1982-2006, the lowest pressure at formation was 999 mb. Second, we included the VR2 term to eliminate the tendency of storm chasing. After the formation of a TC, the 850 mb relative vorticity increases as the 850 mb winds increase; by adding the VR2 term, we tried to account for the negative impact an established TC has on the likelihood of formation of another TC.

We also chose to use 40 percent of the NTCI when developing our logistic regression. When we used 100 percent NTCI, we had indications that the model was drastically under-predicting. As mentioned above, this under-prediction is due to the LSEFs being similar around the TC formation day. Using 40 percent NTCI, we excluded some of the grid points associated with already formed, or about to form TCs. As a result, the LSEFs present on formation day are associated in the regression model with a higher probability of formation than

when 100 percent of the NTCI is used. This greatly reduced our under-prediction problem and improved the model's reliability, as shown in Section B, Chapter III.

Our model faced two challenges because it was trained on data with daily resolution. The training data only includes 273 TCs that formed between 1982-2006 out of 722,850-day grid blocks in the training period. Thus, there is a 0.00037 probability of developing a TC at any day grid block during the training period. Therefore, the daily probability for TC formation is extremely low. As in the WNP, these daily probabilities seldom exceed 5 percent, even in the most favorable regions (Mundhenk 2009). The model-predicted daily formation probabilities are often much higher than these overall average probabilities, but they are still low from the perspective of many forecast users (for example, much less than 50 percent). This raises the challenge of how to present long-range forecasts in which the formation probabilities are generally well below the probabilities at which mission planners are accustomed to revising their plans. .

The second challenge associated with training on daily data is that skillful long lead forecasts of conditions on an individual day are very difficult to produce. To have skill at long lead times, long-range forecasts are generally time averages that are valid over a range a number of consecutive days (e.g., a whole season, month, or week). This time averaging reduces the temporal resolution, but increases the skill, of the forecast. This is in part because a time averaged forecast reduces the impacts of timing errors by expanding the temporal size of the forecast target (e.g., to score a hit, a TC needs to form on just one day during the seven day period, rather than on just the one day on which the TC occurred).

To remedy these problems, we investigated summing the daily probabilities over three-, five-, and seven-day periods. The summed probabilities for all of these cases did a decent job depicting TC formation. We ended up using seven-day summed probability forecasts because they provided the greatest skill while still using a relatively short valid period. Figure 14 is an example of a zero lead seven-day summed probability hindcast using R2 and

OISST LSEFs. The days summed for this forecast are 2 September through 8 September 2002 with the forecast centered on 5 September 2002.

The seven-day summed forecasts allow forecasters and mission planners to work with probabilities that: (1) are large enough to be easily interpreted; and (2) span a short enough period to be operationally useful for long range planning (e.g., for planning a one to two week transit of a battle group).

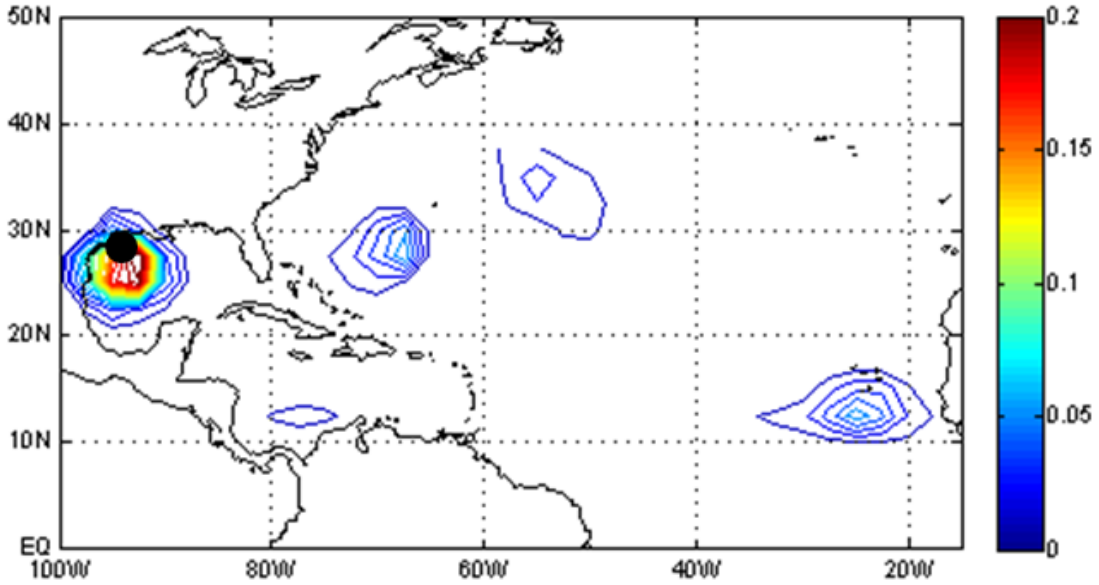

Figure 14. Example of seven-day summed probability from a zero lead hindcast for 2-8 September 2002. The forecast is centered on the 248th day (5 September) of 2002. The black dot represents TC Fay that formed on 5 September 2002. Contours start at 1 percent and are in 1 percent increments. This hindcast was generated using the regression model described at the beginning of Section A, Chapter III, and using 40 percent of the NTCI.

B. VERIFICATION OF THE REGRESSION MODEL

As mentioned above, there is no standard set of verification methods for events as rare as TC formations, so we tested and applied several methods to verify our model.

1. Quantitative Verification

We first used quantitative verification techniques to evaluate our regression model. The reader should consult Wilks (2006) for additional details of the verification techniques used below. We conducted hindcasts for all the years 1982-2006 to test our model and generate a large number of forecasts for verification. We used jackknifing to create our model (see Section 3.c of Chapter II); therefore our zero lead forecasts are independent of the data used to create the forecasts.

All of the verification techniques we used are based on dichotomous observation values, such that a grid point has a value of “one” if a TC occurred or “zero” if no TC occurred. We credited a forecast with a hit at a model grid point, or a “one”, if a TC occurred within a 2.5° radius of the grid point. This 2.5° radius was used to account for uncertainties in HURDAT TC positions, and to account for the spatial scale of the LSEFs and TCs early in their life cycle.

We used the Brier skill score (BSS) to measure the accuracy of our TC probability forecasts. Based on zero lead hindcasts for the peak season, June-November our regression model has a BSS of 0.039589. A 95 percent BSS confidence interval (0.037888 to 0.041508) was created via jackknifing through each of the years in the data set. Though these results are only slightly above zero, it shows that our model has greater skill than climatology.

We also looked at reliability diagrams (e.g., Figures 15-16) to determine the bias in our regression model. If our model was unbiased, the forecasted probability would match the observed frequency. As expected, most of our forecast probabilities are in the 0 to 0.005 bin. The dashed line in Figure 16 depicts a perfectly reliable model and points above the diagonal no skill line represent positive skill. Our model slightly under-predicts below 10 percent as the results are slightly above the dashed perfect reliability line. From these

diagrams, we get a reliability of 0.00003, resolution of 0.0002, and uncertainty of 0.0049. Overall, as with BSS, the reliability diagrams show that our regression model exhibits skill beyond climatology.

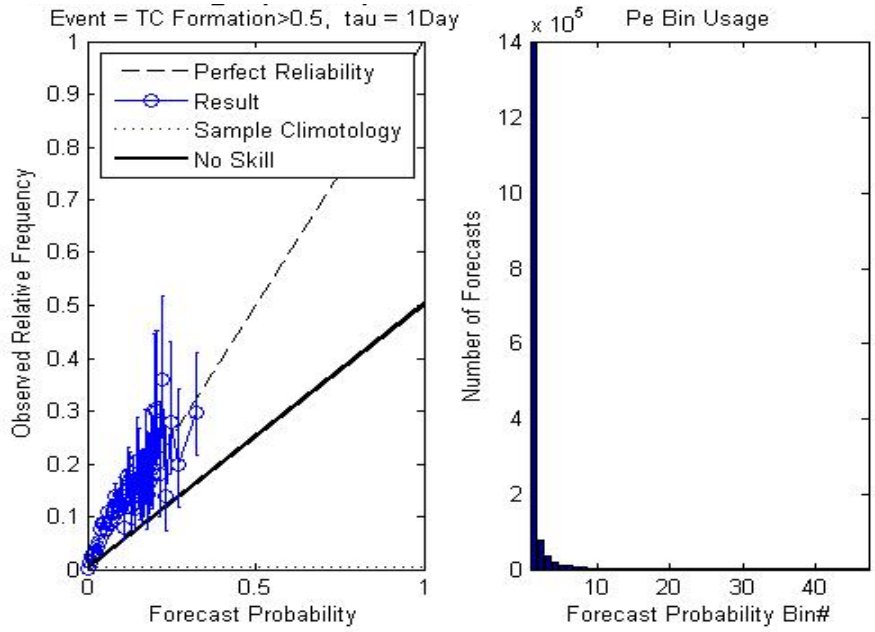

Figure 15. Reliability diagram (left) and the bin histogram (right) for the zero lead hindcasts for June-November of 1982- 2006. Created with minimum bin intervals at 0.005. The error bars on the reliability diagram represent a 95 percent confidence interval.

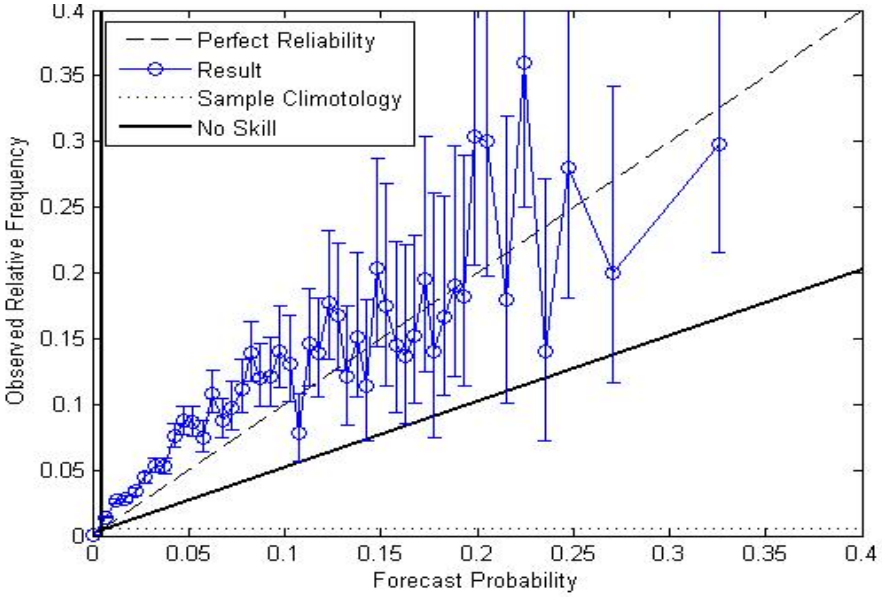

Figure 16. Reliability diagram (left) for probabilities of 40 percent or less for the zero lead hindcasts for June-November of 1982- 2006.

A more familiar way to verify a forecast is looking at the hit rate and the false alarm rate. The relative operating characteristic (ROC) is a graphical tool to analyze both rates simultaneously. Figure 17 depicts a ROC for our zero lead hindcasts. The dashed line in red represents a model with zero resolution, while the red circle at (0,1) represents a model with perfect resolution. As one can see, our model shows good resolution and offers value to the user. We also calculated the ROC skill score (ROCSS), which has a value of one for a perfect forecast and less than zero for a forecast worse than climatology. The ROCSS for our hindcasts is 0.72026, which again shows that our regression model does better than climatology.

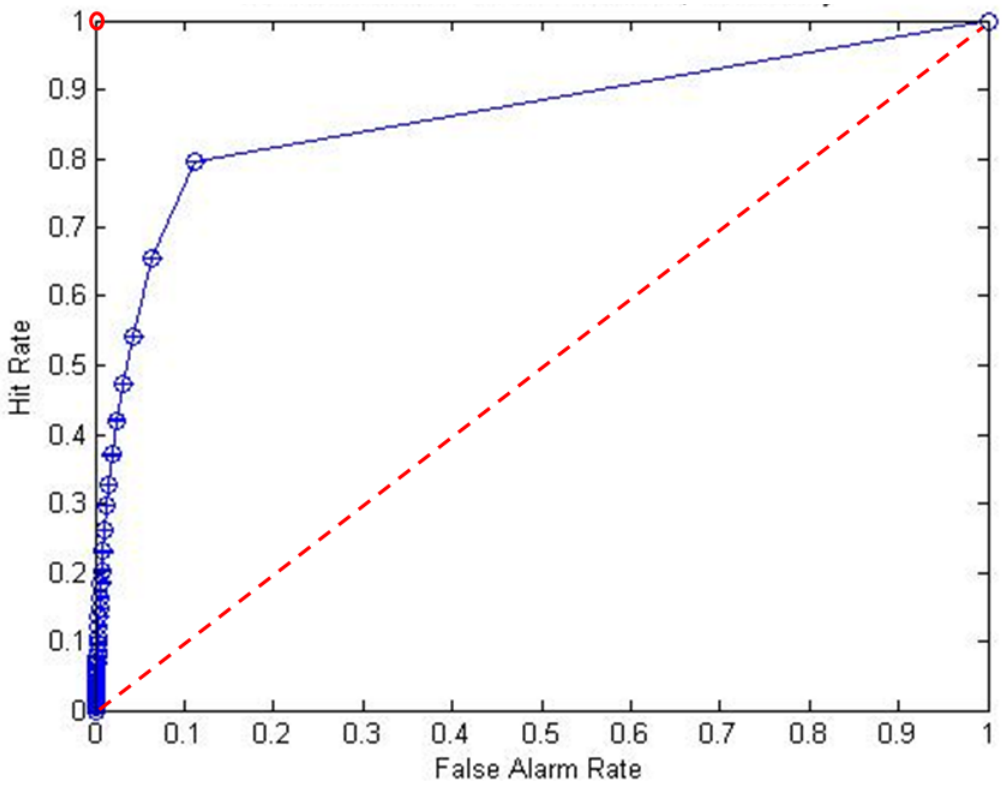

Figure 17. ROC diagram for the zero lead hindcasts for June-November of 1982-2006. The dashed red line represents zero resolution. The red circle at (0,1) represents perfect resolution.

2. Qualitative Verification

We used qualitative verification to compare high formation probabilities generated by the model with actual TC activity. We obtained independent data by skipping a year, or jackknifing, during model development or using data from after the 1982-2006 period used to develop the model. Figure 18 depicts a zero lead independent hindcast for 13 August 2000, developed from a 40 percent NTCI model that jackknifed the year 2000. As one can see, the model shows seven to 8 percent probabilities for the TC formation location, indicating a model hit for this TC.

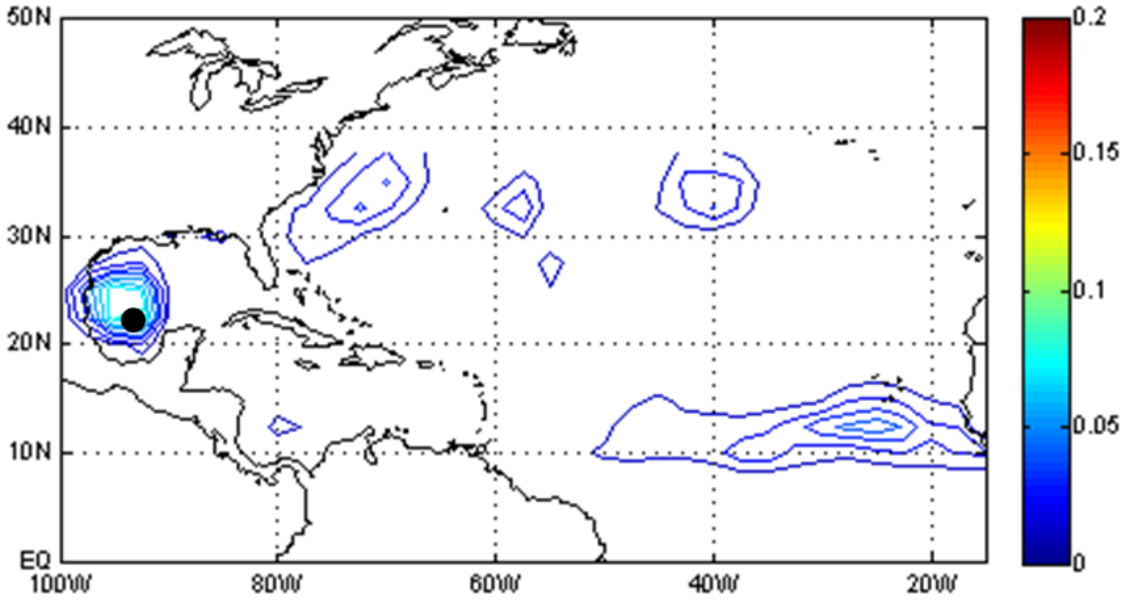

Figure 18. Zero lead seven-day summed TC formation probability hindcast centered on the 226th day (13 August) of 2000, constructed from a 40 percent NTCI model that jackknifed year 2000. The black dot represents TC Beryl that formed on 13 August 2000. Contours start at 1 percent and are in 1 percent increments.

Figure 19 depicts a zero lead hindcast from R2 and OISST fields for 5 November 2008. The years 2007 and 2008 are not included in our regression model because: (1) the R2 data for some of those years was not available at the beginning of our research, and (2) to retain an independent data set for testing

and verification. As one can see, the zero lead hindcast on 5 November 2008 captures TC Paloma at 15 percent, indicating a model hit for this TC.

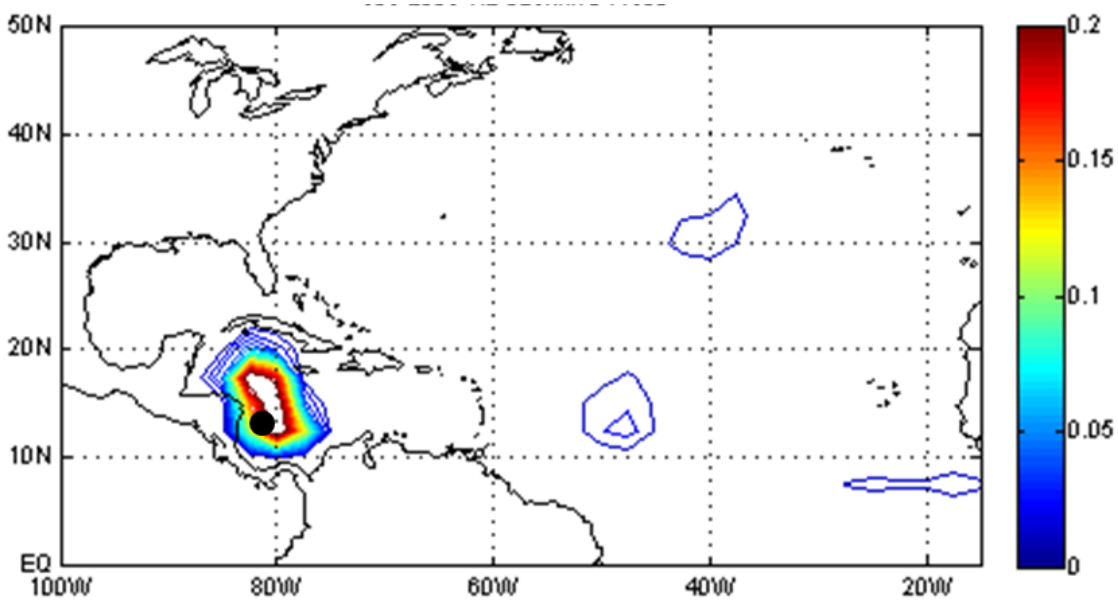

Figure 19. Zero lead seven-day summed TC formation probability hindcast centered on the 309th day (5 November) of 2008, constructed from a 40 percent NTCI model. The black dot represents TC Paloma that formed on 5 November 2008. Contours start at 1 percent and are in 1 percent increments.

3. Comparisons to Climatology

To verify our hindcasts, we also compared model probabilities to those based on climatology. Prior to this study, no probabilistic TC formation climatology was available for the NA. Figure 20 depicts the daily probability that a TC will form at a given grid point; note that the highest value is 0.0666 percent. In scoring hits and misses for our forecasts with respect to climatology, we gave the model forecasts a hit (miss) if the model's daily forecast probability was greater (less) than the climatological probability. Using this method, the model scored 273 hits and 16 misses, for a hit rate of 94.5 percent.

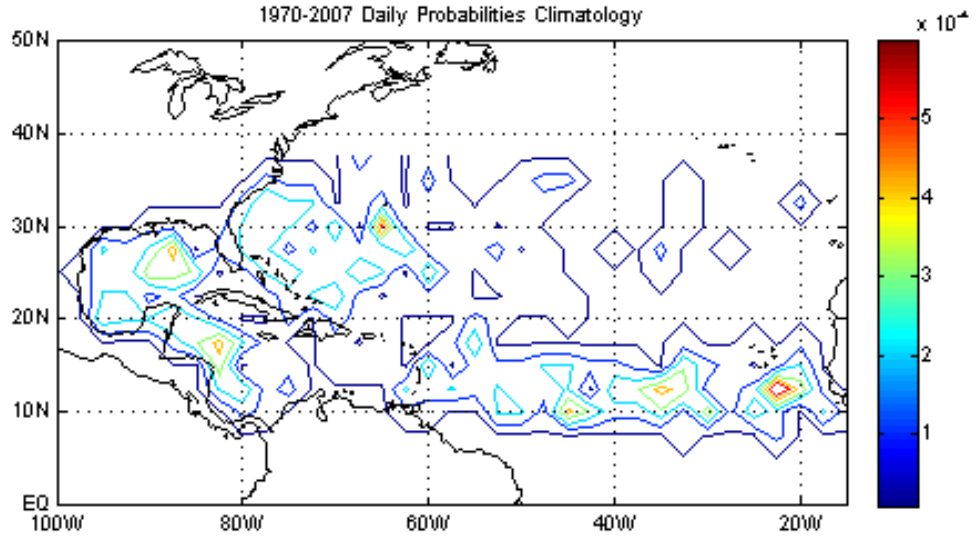

Figure 20. Contoured daily climatology probability of TC formation, constructed from HURDAT from the years 1970-2007. Values represent the daily probability, averaged over the entire year, that a TC will form in a given grid point.

A weakness in the raw spatial climatology shown in Figure 20 is that it has the same values for 1 June as 1 October, which is not consistent with actual TC activity. We would expect the probability for TC formation to be higher on 1 October than on 1 June.

As described by Mundhenk (2009), we created a more robust form of climatology for the NA that varies spatially and temporally. Figure 21 displays the daily probabilities for 1 June and 1 October. As expected with our robust climatology, the daily probabilities for 1 October are higher than the probabilities for 1 June. We used this spatially and temporally varying climatology for the anomaly forecasts below.

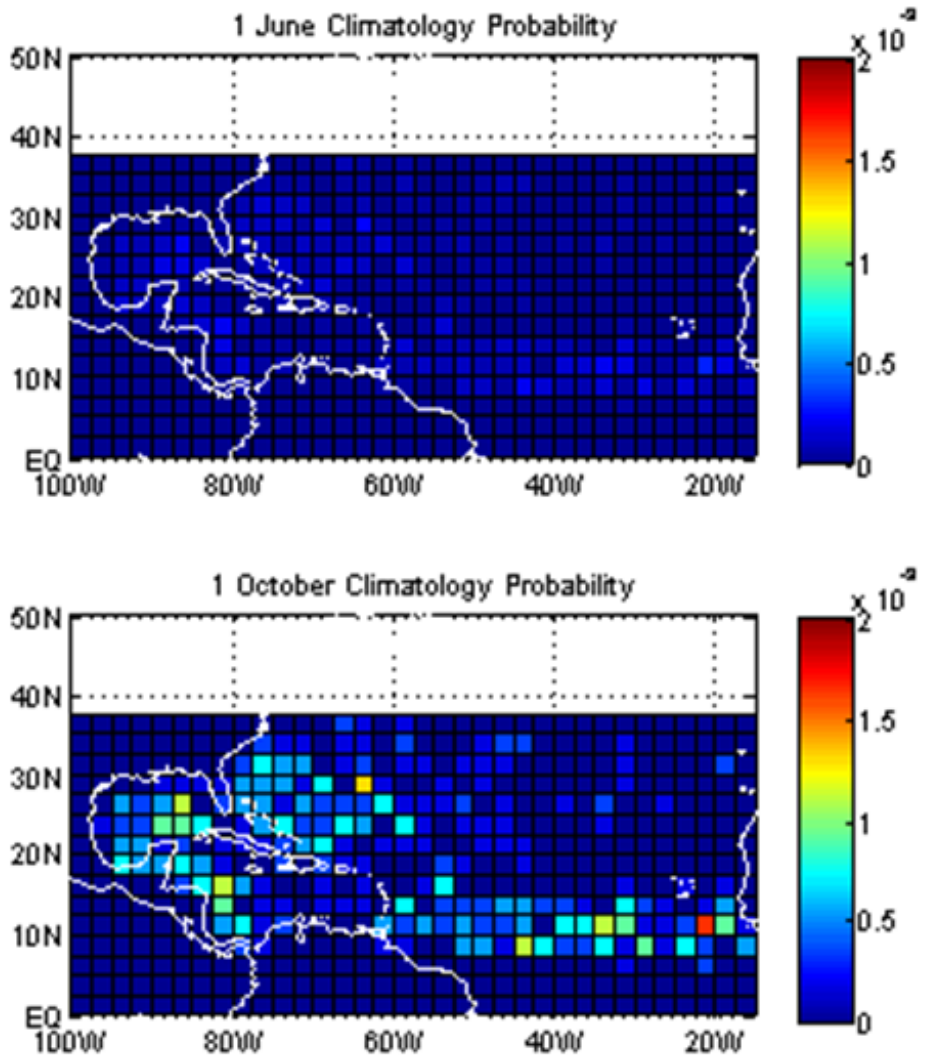

Figure 21. Daily climatology probability of TC formation on 1 June (top) and 1 October (bottom), constructed from HURDAT from the years 1970-2007. Values represent the daily probability that a TC will form in a given grid point.

Figure 22 is similar to Figure 19 but is shows the corresponding forecast anomaly, which is the hindcast probability minus the corresponding robust daily climatology described above. In the anomaly forecast, positive (negative) values indicate regions of above (below) average formation probabilities. Positive and negative anomaly probabilities have potential value in operational planning, since

they identify areas where elevated risks might preclude operations, and areas where suppressed risks might provide opportunities for operations that do not normally exist.

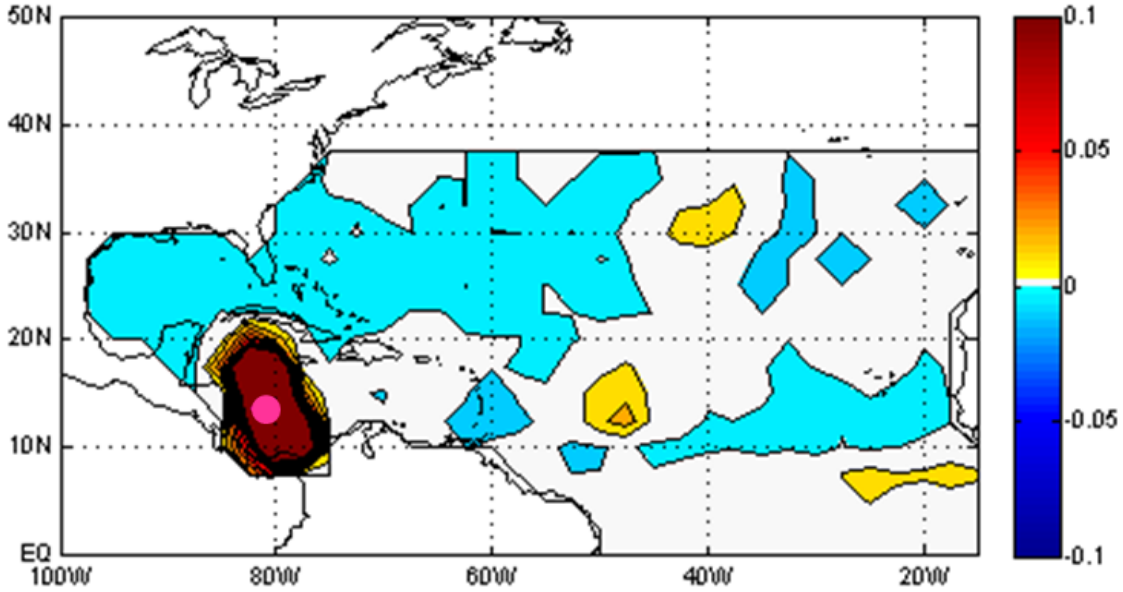

Figure 22. Zero lead seven-day summed TC formation probability hindcast anomaly calculated as seven-day summed hindcast probability minus seven-day summed robust daily climatology probability. Centered on the 309th day (5 November) of 2008 and constructed from a 40 percent NTCI model. The magenta dot represents TC Paloma that formed on 5 November 2008.

4. Verification Against Deep Convection

Our model appears to do quite well at predicting tropical convection as well as TC formation, similar to the results of Mundhenk (2009) for the WNP,. We chose to verify our model against outgoing longwave radiation (OLR), since low OLL values highlight deep convection, which in turn indicate areas that are favorable for TC formation. Figure 23 shows an example of this verification for the six-week lead forecast probabilities for 13 Nov 2008 compared to the analyzed OLR on the same day. For this non-zero lead forecast, we used forecasts of the LSEFs from CFS to force the regression model (as discussed in Chapter II). Note that off the coast of Panama, there was a region of high probabilities, which coincided with an area of low OLR (cool colors). In this case,

there was not TC formation in the Panama region, but occurrence of deep convection in the region indicates that the model correctly identified deep convection conditions that tend to be favorable for TC formation (Gray 1968, 1975, 1979). These and similar results for other cases indicate that our model has potential for forecasting tropical convection at intraseasonal lead times (six weeks in this example).

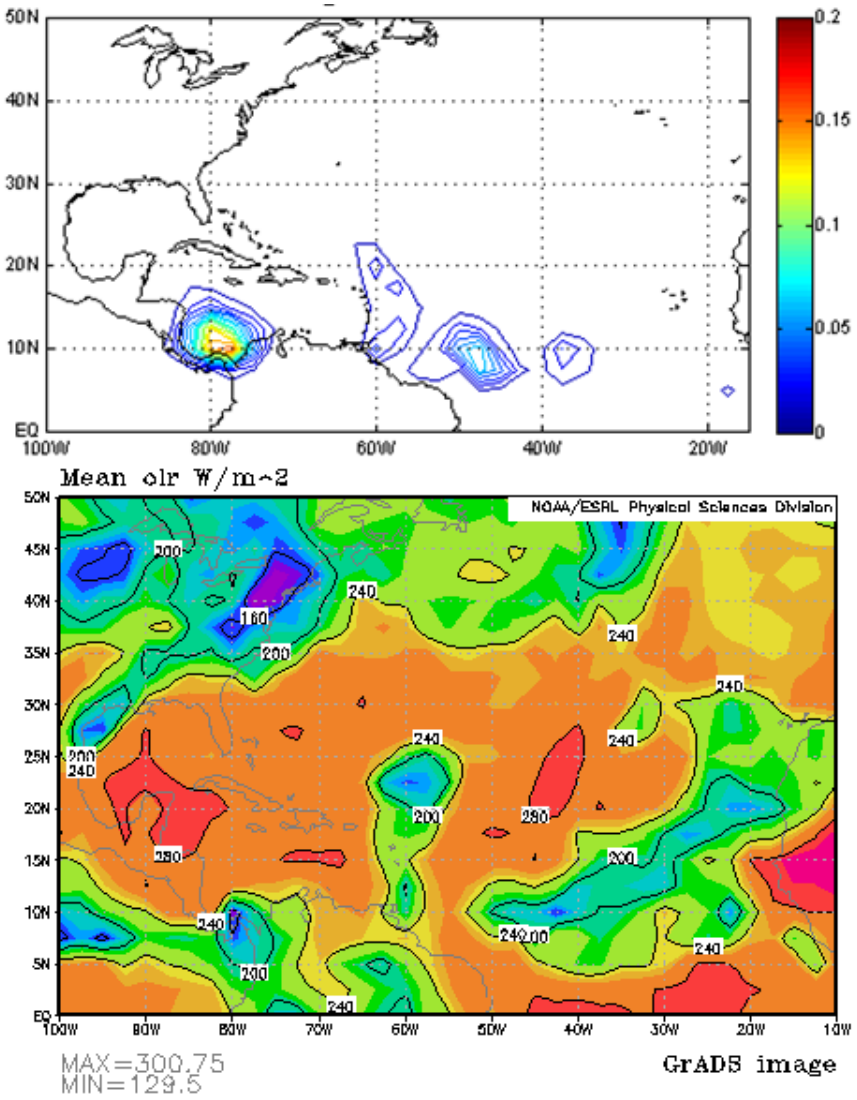

Figure 23. Comparison of a six-week lead forecast probabilities (top) and OLR (bottom) for 13 November of 2008. OLR image provided by Physical Sciences Division (PSD), Earth System Research Laboratory, NOAA, Boulder, Colorado (PSD 2008).

C. FINDINGS FROM CFS CASE STUDIES

We conducted six non-zero lead hindcast studies from our archived CFS data. All of six cases showed promising results, and the results from two of the cases are summarized in this section.

1. Non-Zero Lead Hindcasts: Paloma

TC Paloma formed off the east coast of Nicaragua on 5 Nov 2008 and, according went on to become the second-strongest November hurricane on record in the NA (NHC 2009). Figure 24 depicts the zero lead hindcast using R2 LSEFs (panel a) and the one through seven week lead hindcast probabilities created via our model when forced with CFS forecasts of the LSEFs (panels b-h).

Figure 24 shows that the zero lead hindcast has higher probabilities than the one to seven week lead hindcasts. This result holds for all of our case studies. This is one of several indications, compared to the R2 LSEFs, the CSF LSEFs have trouble capturing smaller spatial structures and intensities in the LSEFs. However, the one-week forecast from the CFS does a great job depicting TC Paloma with a 20 percent probability centered on the formation location.

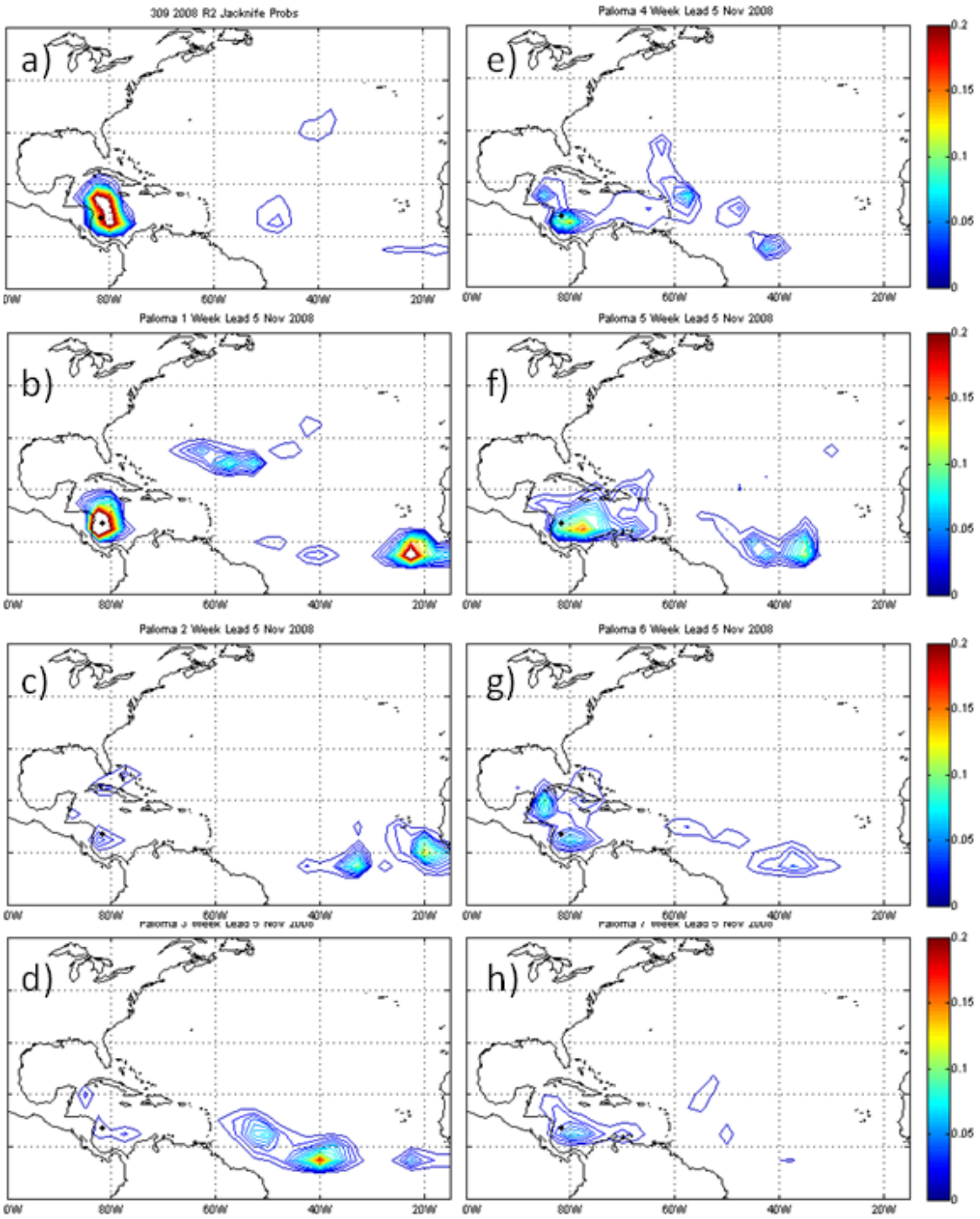

Figure 24. Comparison of seven-day summed probabilities of TC Paloma centered on 5 November 2008 from: (a) zero lead hindcast forced by R2 LSEFs; and (b) one to seven week lead hindcasts forced by CFS LSEFs. Contours start at 1 percent and are in 1 percent increments.

Figure 24 also shows that all the non-zero lead hindcasts depict TC Paloma within a 1 percent probability contour. Weeks two and three are the worst, with a two and 1 percent probability contour around the formation location. Weeks four and five depict TC Paloma within seven and nine percent probability contours, respectively. Week six depicts TC Paloma within a four percent probability contour. Week seven only depicts TC Paloma within a three percent probability contour, but we think it is perhaps the most promising of the non-zero lead hindcasts because: (1) it captures Paloma at a long lead time; and (2) it does so within a relatively confined and specific region east of Nicaragua. . of the out creating . This result indicates that forecasts based on our model and CFS LSEFs can have sufficient skill to make them useful in operational planning at relatively long leads (e.g., at a lead of one to two months, military planners would be advised to try to avoid operations in the Mosquito Gulf).

Figure 25 shows the zero lead and seven week lead hindcasts of the 850 mb relative vorticity and the 200 mb divergence LSEFs that correspond to the hindcasts shown in Figure 24. Note that the CFS-based seven week lead hindcasts do well in depicting both of these LSEFs in the TC Paloma formation region, which leads to relatively accurate hindcast probabilities. But, as expected, the zero lead hindcast based on R2 LSEFs depicts a greater level of spatial structure at the two levels when compared to seven-week lead hindcast.

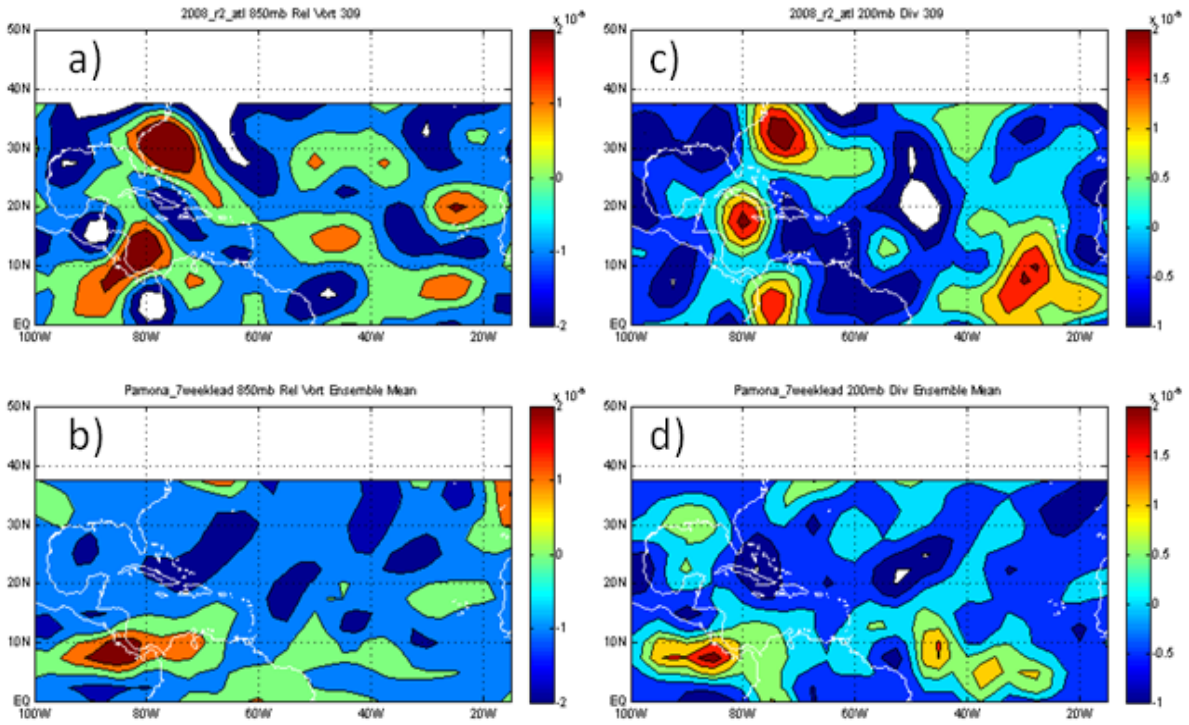

Figure 25. Comparison of 850 mb relative vorticity (panels a and c, in /s) and 200 mb divergence (panels b and d, in /s) for: (a and b) zero lead hindcasts based on R2 LSEFs; and (c and d) seven-week lead hindcast based on CFS LSEFs. Both hindcasts valid on 5 November 2008. Corresponding TC formation probability hindcasts shown in Figure 24.

Figure 26 compares for the TC Paloma hindcasts the 850 mb relative vorticity for the one-week and seven-week hindcasts. Note that the one-week lead hindcast depicts a greater level of spatial structure that may contribute to the greater accuracy of the one-week lead hindcast.

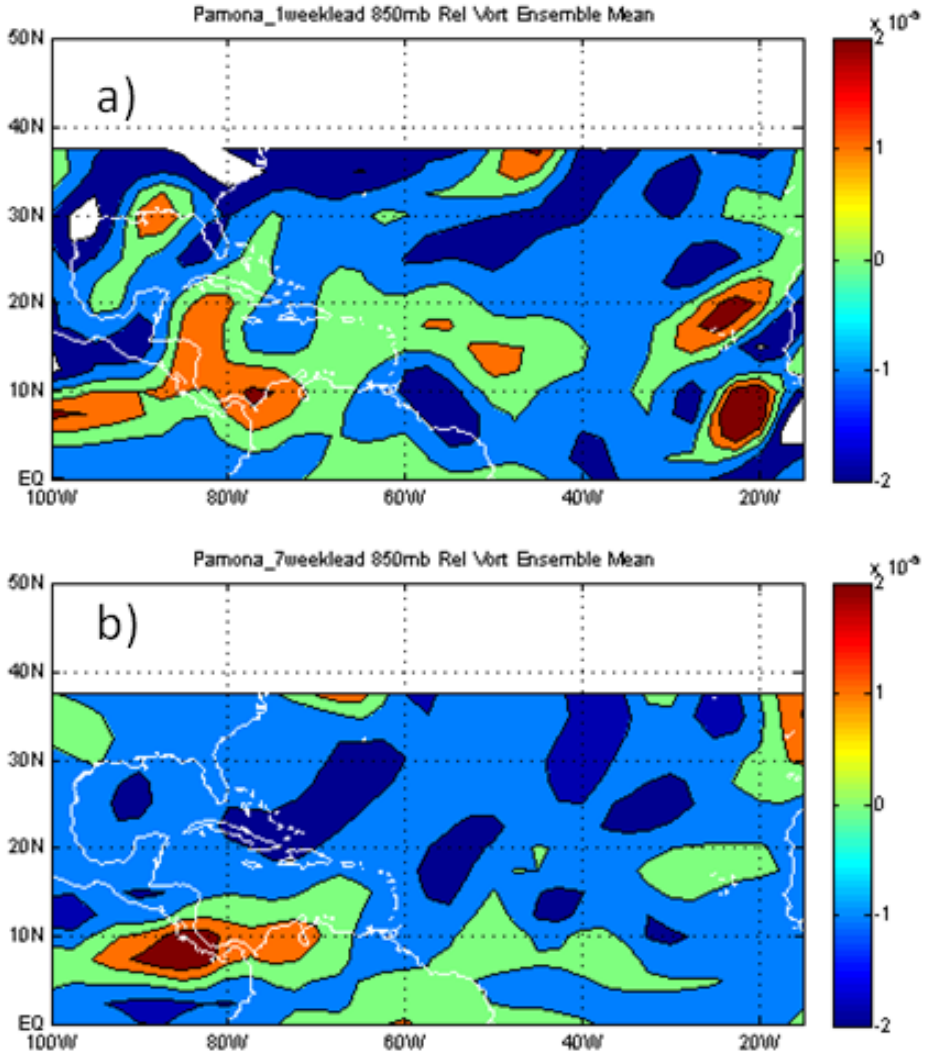

Figure 26. Comparison of 850 mb relative vorticity for: (a) one-week lead hindcast; and (b) seven-week lead hindcast, with both hindcasts based on CFS LSEFs and valid on 5 November 2008. Corresponding TC formation probability hindcasts shown in Figure 24.

2. Non-Zero Lead Hindcasts: Omar

TC Omar was an interesting case to study because the NA had a complex pattern of TC activity. TC Omar formed on 13 October 2008, but TC Nana formed the day before and TD 16 formed the day after. Figure 27 depicts the seven day summed formation probabilities for the zero to four-week lead hindcasts centered on 13 October 2008.

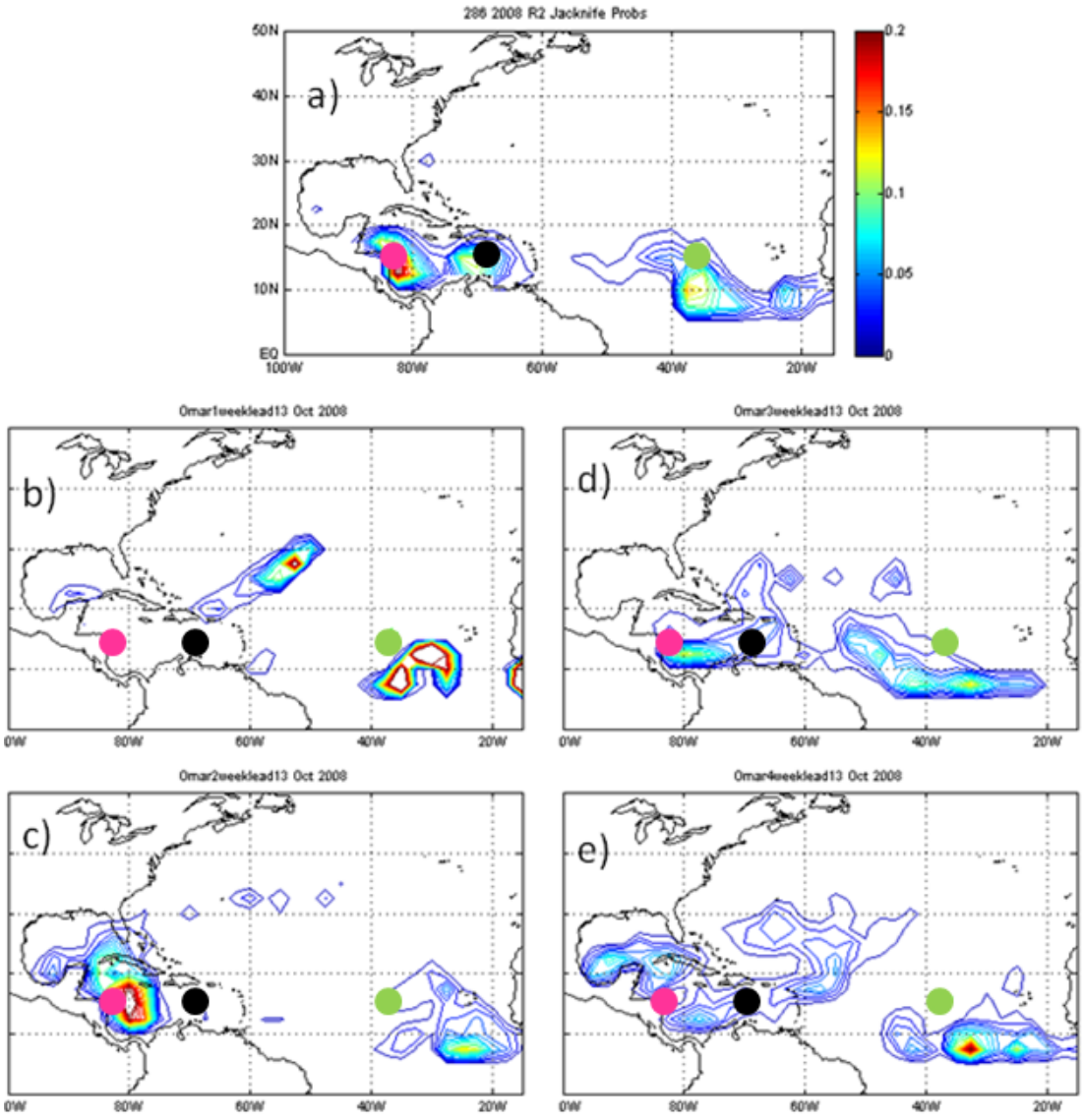

Figure 27. Comparison of seven-day summed probabilities of TC formation centered on 13 October 2008 from: (a) zero lead hindcast forced by R2 LSEFs; and (b) one-week, (c) two-week, (d) three-week, and (e) four-week lead hindcasts forced by CFS LSEFs. Contours start at 1 percent and are in 1 percent increments. The formation locations are depicted by the colored dots: black dot for TC Omar (formed on 13 October 2008); green dot for TC Nana (formed on 12 October 2008); and magenta dot for TD 16 (formed on 14 October 2008).

Unlike TC Paloma, the one-week lead hindcast for TC Omar did not perform well at all, in fact all three storms were missed at this lead time. The two-week lead hindcast represents TD 16 within a 13 percent contour, but it still

does not predict TC Omar. The best results for Omar are from the three-week lead hindcast, with the formation location within the four percent contour (Figure 27, panel d). For TD 16, the best results are from the two-week lead hindcast, but the highest probabilities are to the southeast of the formation point.

Having the highest probabilities to the southeast of the corresponding formation point is a problem in many of our results. This problem occurs not just in the non-zero lead hindcasts based on the CFS LSEF forecasts, but also in the zero lead hindcasts based on the R2 data. This problem is likely due to the TC HURDAT data only starting at TD strength, so that the initial locations of the TCs in the HURDAT data (e.g., the dots shown in Figures 14, 18, 19, 22, 24, 27) are to the northwest of the actual formation locations. If so, then the regression model, combined with the R2 and CFS LSEFs, are able to recognize the favorable conditions that existed prior to the initial HURDAT location for the TCs.

Figure 28 shows the 850 mb relative vorticity used for zero lead R2 based hindcast and the one-week lead CFS based hindcasts shown in Figure 27. The CFS does not capture the positive 850 mb relative vorticity in the TC Omar and TD 16 vicinities. Figure 29 shows that the CFS also does an insufficient job in depicting the 200 mb divergence in the TC Omar and TD 16 vicinities. These CFS shortcomings lead, in this case, to insufficient formation probabilities for TC Omar and TD 16.

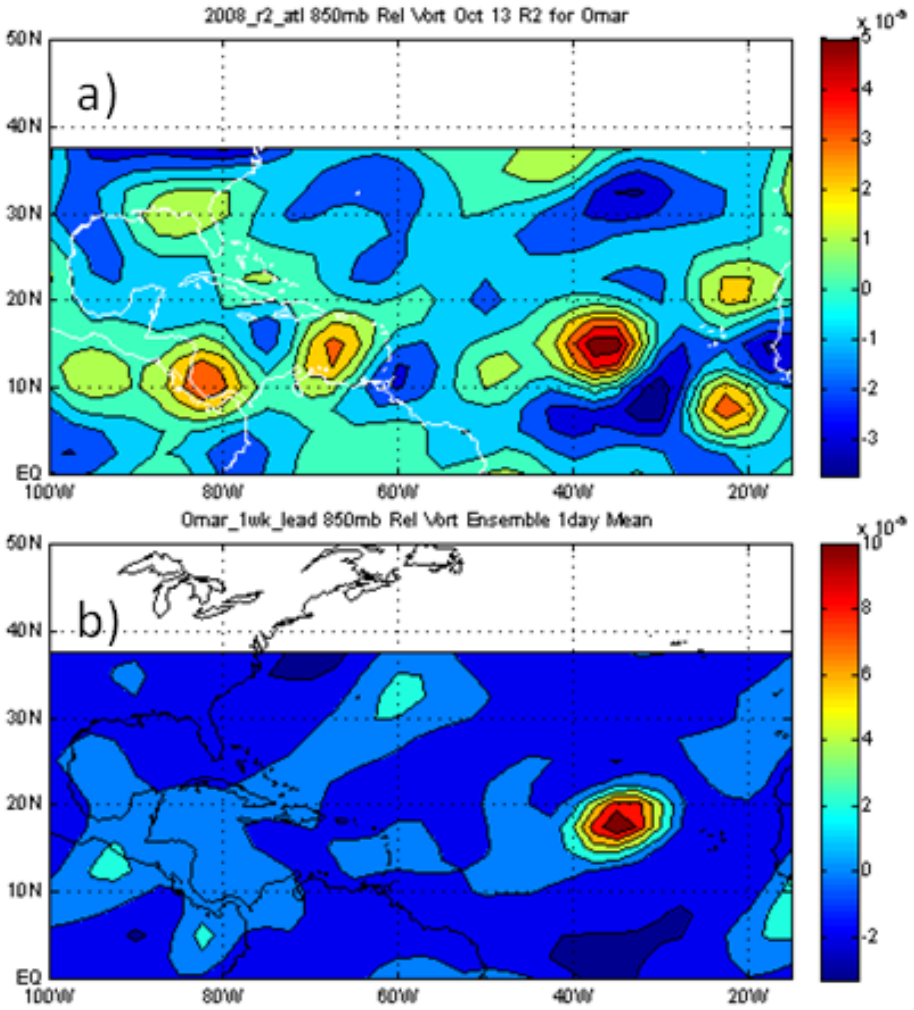

Figure 28. Comparison of 850 mb relative vorticity for: (a) zero lead hindcast based on R2 LSEFs; and (b) one week lead hindcast based on CFS LSEFs, valid on 13 October 2008. Corresponding TC formation probability hindcasts shown in Figure 27.

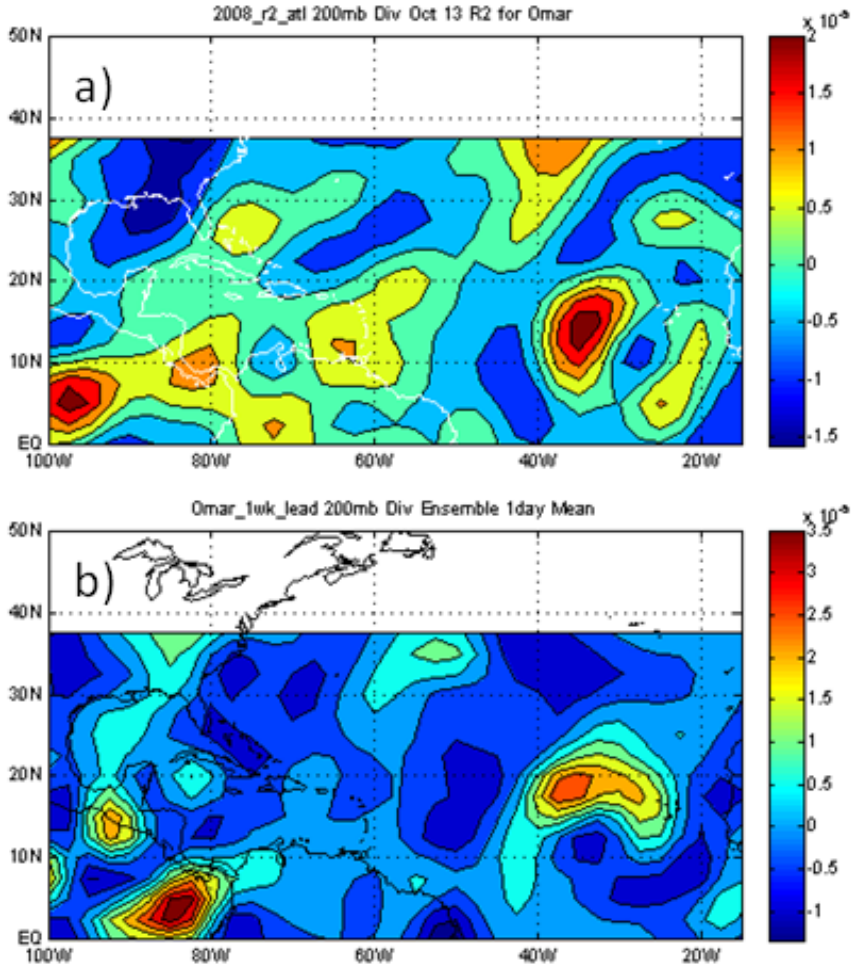

Figure 29. Comparison of 200 mb divergence for: (a) zero lead hindcast based on R2 LSEFs; and (b) one week lead hindcast based on CFS LSEFs, valid on 13 October 2008. Corresponding TC formation probability hindcasts shown in Figure 27.

The formation probabilities for TC Omar at the two-week lead time (not shown) are just as poor as the one-week lead time due to a poor depiction by the CFS of the 850 mb relative vorticity and 200 mb divergence. However, the corresponding formation probabilities for TD 16 (not shown) do a better job than the one-week lead. At the three and four-week lead times, the CFS does well at depicting both 850 mb relative vorticity and 200 mb divergence, leading to good representation of TC Omar and TD 16 in the corresponding formation probabilities.

Figure 30 shows for TC Omar three-week lead hindcast formation probability anomaly (see Section 3 of Chapter II for more on these anomalies). This figure shows that TC Omar and TD 16 occurred within areas that the hindcast identified as having above average formation probabilities. Thus, the three-week lead hindcast represents an improvement over the use of climatological probabilities. The similarities between the formation probability anomalies shown in Figure 30 and the corresponding formation probabilities shown in Figure 27, panel d, indicate that the formation probabilities in Figure 27, even the probabilities of just a few percent, represent probabilities that exceed the average probabilities for this seven-day period. This is generally true of the hindcast and forecast probabilities.

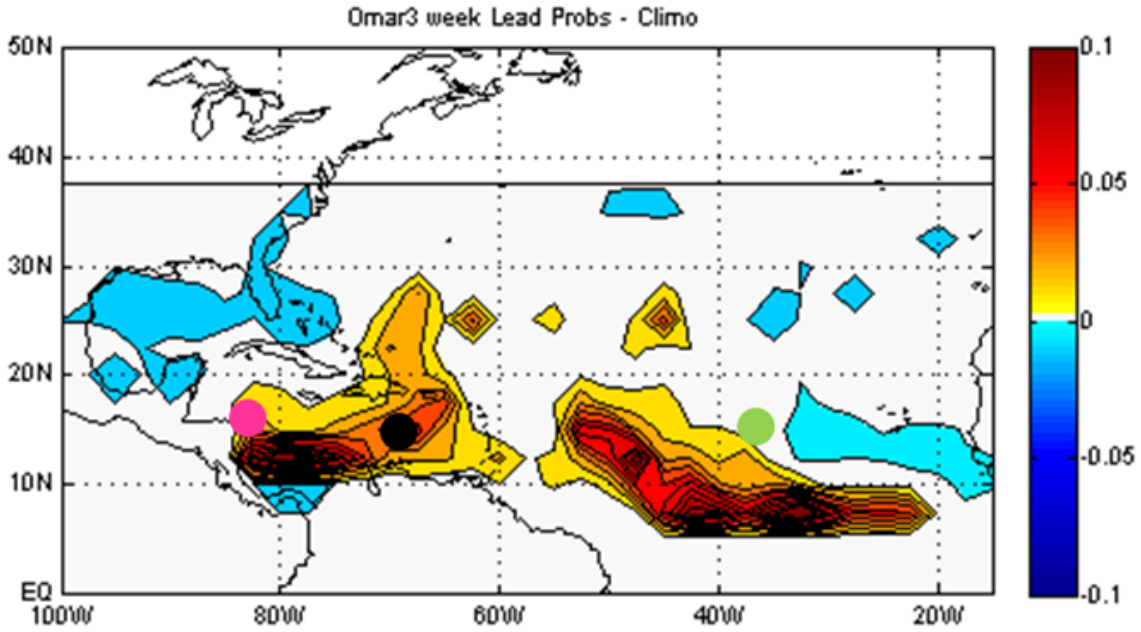

Figure 30. Three-week lead seven-day summed TC formation probability hindcast anomaly centered on 13 October 2008. The black dot represents TC Omar that formed on 13 October 2008, the green dot represents TC Nana that formed on 12 October 2008, and the magenta dot represents TD16 that formed on 14 October 2008. Compare this figure to the corresponding formation probability hindcast in Figure 27, panel d.

3. CFS Two-week Forecast Comparison

In an operational sense, our model needs to be consistent from day to day. If a two-week CFS forecast initialized on 14 May (forecast probabilities centered on 29 May) accurately predicts high probabilities near Cuba, then a two-week CFS forecast initialized on 15 May (forecast probabilities centered on 30 May) should also predict high probabilities in that region. A lack of such consistency is an indication of not only scientific problems with the forecasting system but also of potential problems in using the forecasts in planning operations. Inconsistent forecasts indicate forecast uncertainty and makes it difficult to confidently develop plans based on the forecasts.

To check for day-to-day consistency in our forecasts, we created seven two-week forecasts initialized a day apart from one another; the first initialized on 26 September 2008 (forecast probabilities centered on 10 October 2008), and the last initialized on 2 October 2008 (forecast probabilities centered on 16 October 2008). During this forecast period, TC Nana formed on 12 October, TC Omar formed on 13 October, and TD 16 formed on 14 October. Figure 32 shows the results from these two-week forecasts. Note in this figure the overall consistency from day to day in these seven two-week lead hindcasts. This consistency helps validate our forecast system and its use, and indicates that the forecasts from our system may be consistent enough to be useful to military planners.

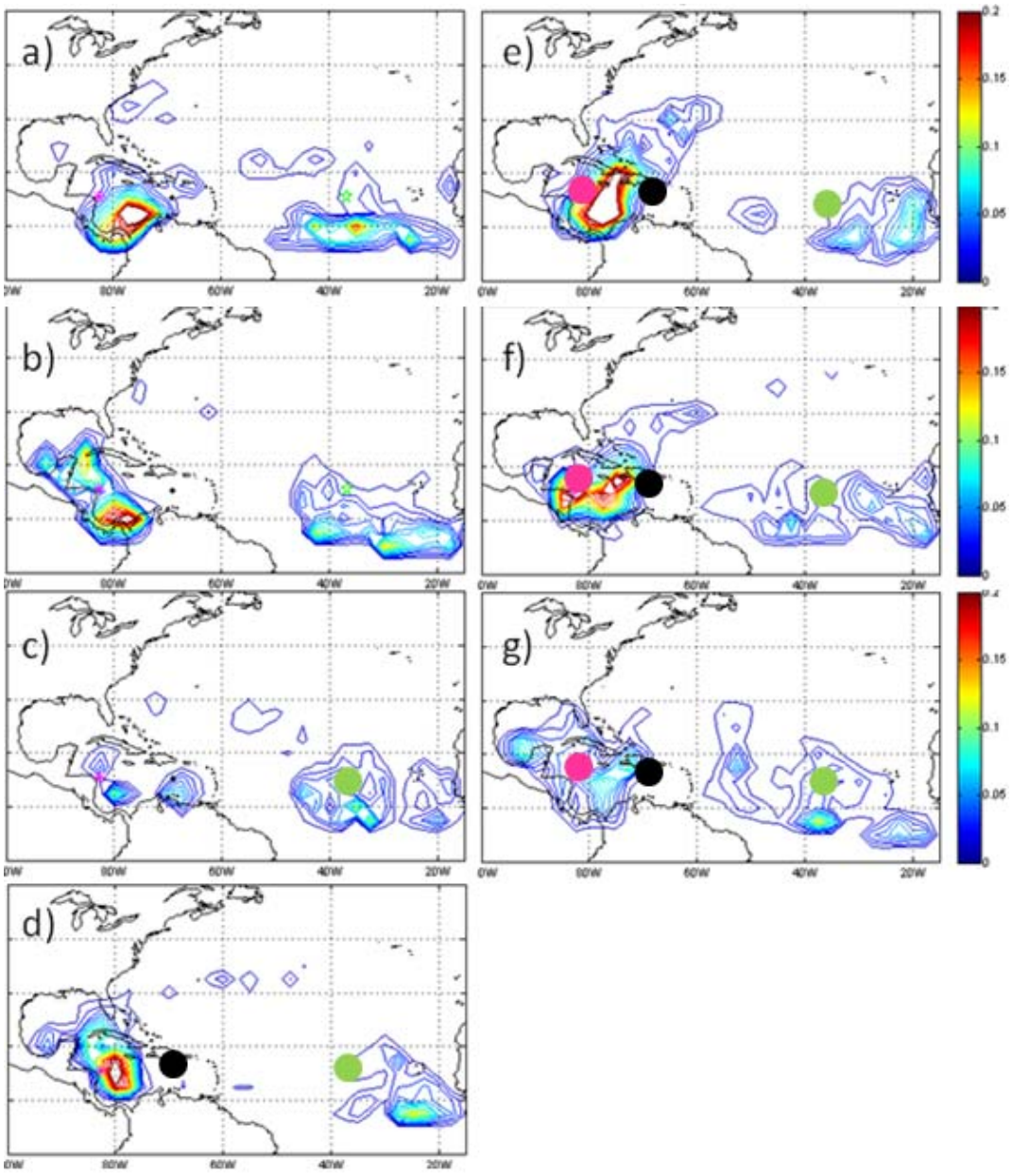

Figure 31. Seven-day summed TC formation probabilities from seven two-week lead hindcasts, valid on: (a) 10 October 2008; (b) 11 October 2008; (c) 12 October 2008; (d) 13 October 2008; (e) 14 October 2008; (f) 15 October 2008; and (g) 16 October 2008. TC Nana (formed on 12 October 2008) is depicted by the green dot, TC Omar (formed on 13 October 2008) is depicted by the black dot, and TD 16 (formed on 14 October 2008) is depicted by the magenta dot. Contours start at 1 percent and are in 1 percent increments. Note the general consistency in the probabilities for forecasts validating on consecutive days.

4. Forecasts for June 2009

In addition to hindcasts, we also generated experimental forecasts for the 2009 NA TC season. Figure 32 below depicts some of these forecasts of TC formation probabilities, all of which were initialized on 20 May 2009. The valid periods are centered on 3, 10, 17, and 24 June 2009 with lead times of two, three, four, and five-weeks, respectively. To the right of each forecast is the corresponding anomaly forecast (see Section 3 of Chapter II). Note that that the forecasted probabilities in Figure 32 are not extremely high. This is consistent with NA TC activity in June generally being low to modest. Note also a general increase in probabilities from the first week to the last week, also consistent with historical TC activity patterns (e.g., Figure 5).

Since the valid periods for the forecasts shown in Figure 32 will occur after the writing of this report, the verification of these forecasts is beyond the scope of this study. However, readers may verify these forecasts using TC data information at http://www.nhc.noaa.gov/pastall.shtml and OLR data at http://www.cdc.noaa.gov. The verification of these forecasts will be useful in assessing the potential value of such forecasts to military planners.

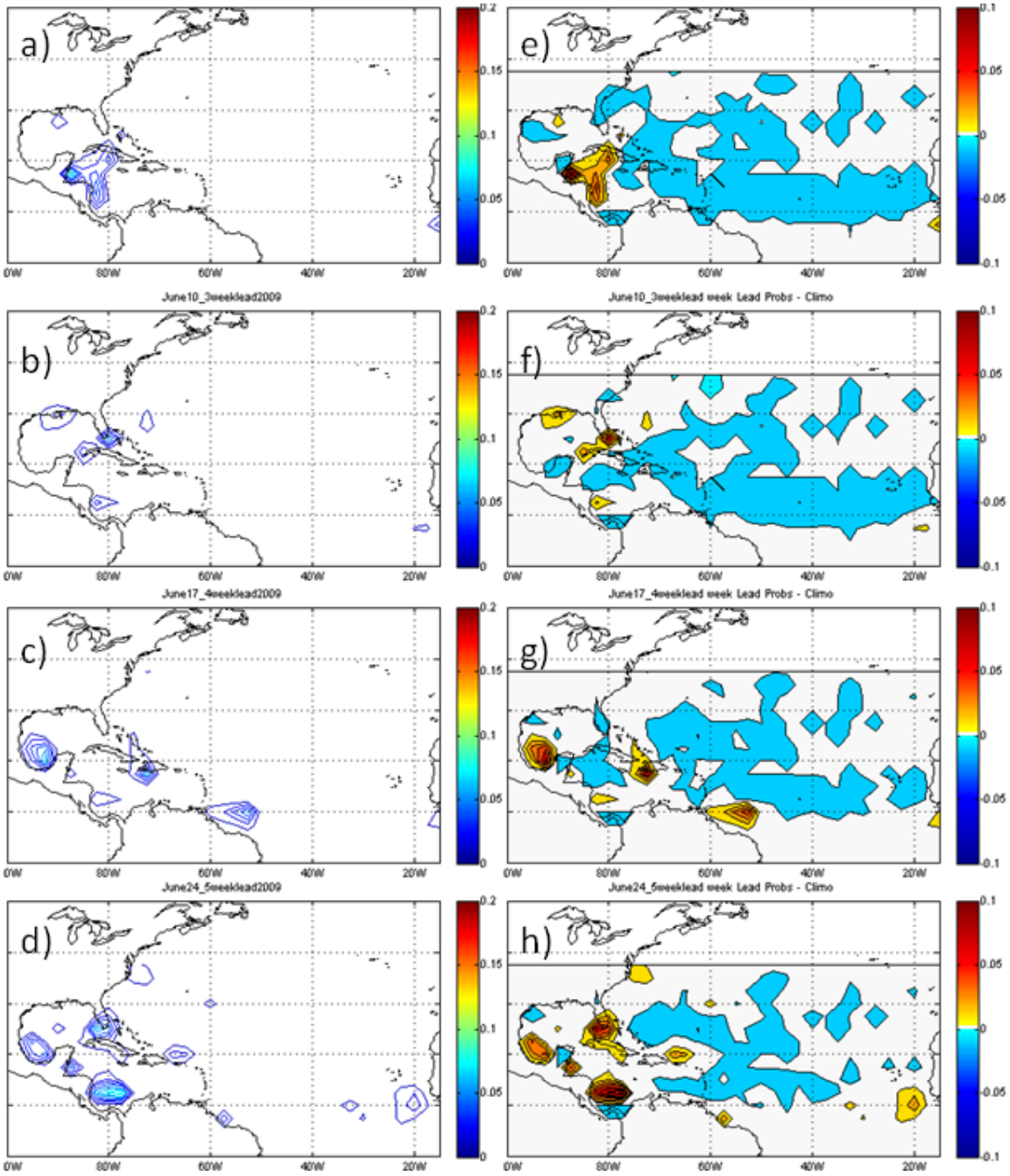

Figure 32. Seven-day summed TC formation probability forecasts (left column) and TC formation probability forecast anomalies (right column) from four forecasts initialized on 20 May 2009 and valid on: (a) 03 June 2009; (b) 10 June 2009; (c) 17 June 2009; (d) 24 June 2009. Contours start at 1 percent and are in 1 percent increments.

5. Forecasts for July 2009

Figure 33 shows forecasts of TC formation probabilities. initialized on 20 May 2009 and valid for the seven day periods centered on each Wednesday of July 2009 (i.e., 1, 8, 15, 22, and 29 July 2009). To the right of each forecast is the corresponding anomaly forecast (see Section 3 of Chapter II). Note that that the forecasted probabilities in Figure 32 are not extremely high. This is consistent with NA TC activity in June generally being low to modest. Note also a general increase in probabilities from the first week to the last week, also consistent with historical TC activity patterns (e.g., Figure 5).

The LSEFs in July, compared to June, should be more favorable for TC formation; therefore, we should see higher probabilities in July. In fact, the forecasted July 2009 probabilities are higher than those for June 2009 and indicate that more of the NA is favorable for TC development. The increase in favorable areas is especially noticeable in the main development region for NA TCs, the tropical Atlantic between northern South America and western North Africa (see Section B.1 of Chapter II). This is consistent with historical TC activity, with July having experienced during 1970-2007 almost twice as many TC formations as June (see Figure 5). As discussed in the prior section, we leave it to the reader to verify these forecasts.

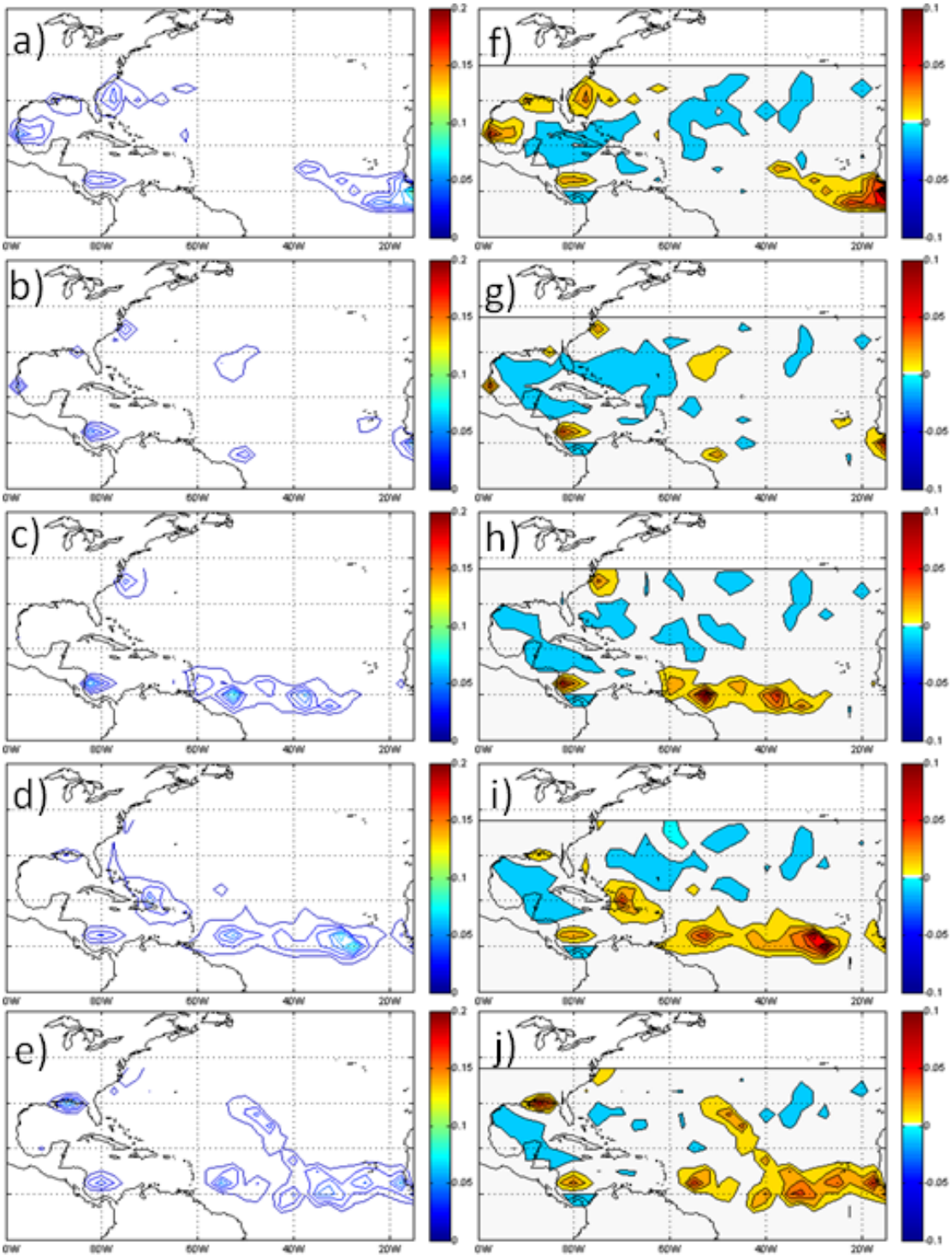

Figure 33. Seven-day summed TC formation probability forecasts (left column) and TC formation probability forecast anomalies (right column) from five forecasts initialized on 20 May 2009 and valid on: (a) 01 July 2009; (b) 8 July 2009; (c) 15 July 2009; (d) 22 July 2009; and (e) 29 July 2009. Contours start at 1 percent and are in 1 percent increments.

6. General Observations

We have shown that using the R2 data, we can skillfully hindcast at zero lead times the formation times and locations of individual TCs at intraseasonal lead times. To hindcast or forecast at non-zero lead times, we need accurate long range forecasts of the LFESs to force our regression model. The CFS appears to have potential for producing these LSEF forecasts. Our results indicate that the skill of the CFS forecasts may be somewhat more consistent at lead times longer than three-weeks than at shorter lead times. We suspect that this difference in consistency may be due to a greater tendency at shorter leads for the CFS to depict the small=scale circulations associated with individual TCs, which then lead to high formation probabilities from the regression model. If so, and if these circulations are inconsistently forecasted by the CFS (as seems likely), then the shorter lead formation probability forecasts will also be inconsistent. At longer lead times, the bias corrected CFS forecasts appear to tend to smooth out the smaller scale circulations and to produce more consistency in forecasting the LSEFs.

A recurring problem in our model is the tendency to forecast high TC formation probabilities north of Panama. As seen in Figure 4, that region has only produced a handful of TCs during 1970-2007. Thus, our model has a tendency to over-predict TC formation probabilities in this region. We tried a few different approaches to correcting this problem that reduced the problem but did not eliminate it. It may be that a bias correction needs to be applied to the model's output for this region. It is useful to note, however, that high probabilities in this region are consistent with a tendency for deep convection in this region during June-November (see Figure 34). Our model highlights this convectively active region and produces high TC formation probabilities as a result.

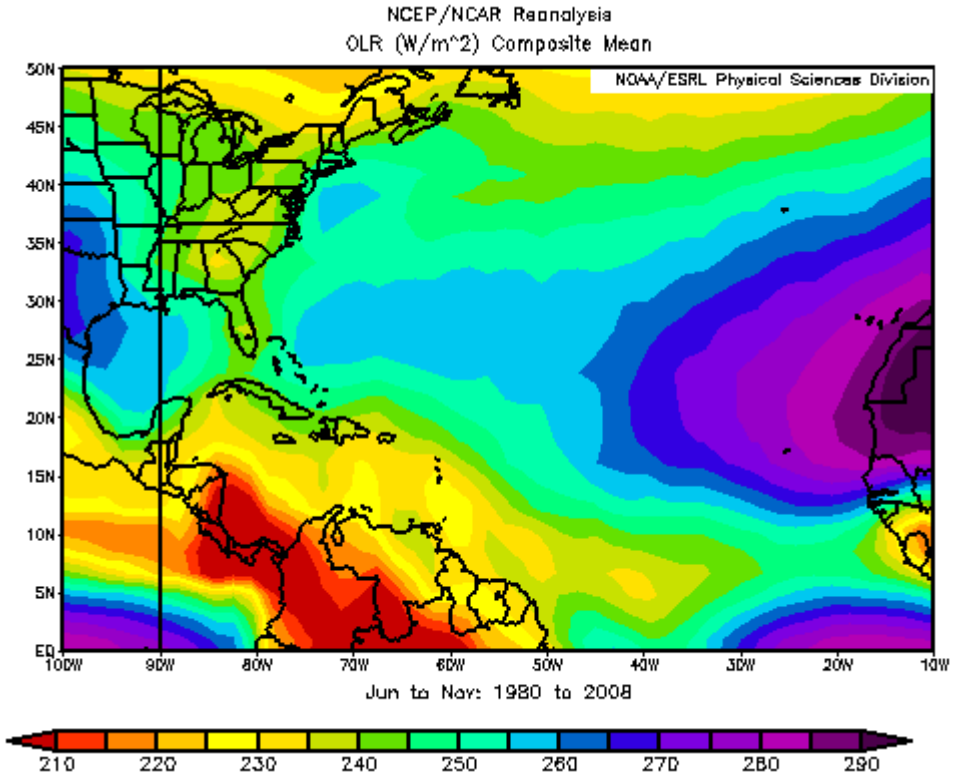

Figure 34. Long term mean ORL for July-November 1982-2008 (PSD 2008).

Another problem with the model is a timing issue, which is probably due to HURDAT. The highest probabilities associated with a given TC tend to occur prior to and to the southeast of the initial HURDAT time and location. As mentioned in Chapter II, HURDAT only has TC data from the time and location at which a TC reached TD intensity. Thus, our model probably tends to identify high probabilities prior to the initial HURDAT date for a TC (i.e., prior to the TC reaching TD intensity).

As with any long lead forecast, with increasing lead times, the skill of the forecast tends to decrease. As mentioned earlier, we addressed this problem by forecasting for seven day valid periods using seven-day summed probabilities.

IV. SUMMARY, CONCLUSIONS, AND RECOMMENDATIONS

A. KEY RESULTS AND CONCLUSIONS

In this thesis, we created and tested a combined statistical-dynamical model to predict the probability of TC formation at daily, 2.5° horizontal resolution in the NA at intraseasonal lead times. We trained the model using R2 and NOAA OISST data, with the results summarized in Table 1. We then forced the model with operational CFS forecasts of the LSEFs. Using the CFS forecasts to force our regression model, we have the potential to predict TC formations at lead times of up to several seasons. However, in this thesis our longest lead time for a verified hindcast or forecast was seven weeks. In this seven-week forecast, our model depicted TC Paloma within the 3 percent contour and above the climatological probability.

During verification of our model, we tested the predictive potential of our model using quantitative and qualitative verification of R2 and NOAA OISST based, zero lead hindcasts. Our model showed great potential with a BSS of 0.0396, a ROCSS of 0.720, and a hit rate of 94.5 percent. We also found that our model verified well against tropical deep convection (as indicated by OLR). This is because the model's TC formation probabilities are closely related to the probability of deep convection in general. This deep convection sometimes leads to TC formation, and other times lead to storms with winds below the TD threshold. From a practical standpoint, for the military planner, areas of elevated tropical cyclone formation probabilities are regions that are good to avoid whether the result is TC formation, or merely deep convection.

We found that the model for the NA is very similar to that for the WNP (Mundhenk 2009). This supports the idea that TCs have similar relationships to LSEFs in all the tropical basins in which TCs they form. It also indicates that eventually one version of our model may apply to all these basins.

We also used our model to produce non-zero lead hindcasts based on CFS predictions of the LSEFs. The skill at leads times greater than two weeks was encouraging However, CFS has difficulty in forecasting the small and intense low level circulations that tend to occur during TC formations. This CFS shortcoming tended to reduce the accuracy of these hindcasts. The most significant weakness of our forecasting system is the inability of CFS to properly forecast small and/or intense features in the LSEFs.

B. APPLICABILITY TO DOD OPERATIONS

There is a gap between existing climate and long range forecasting capabilities and the products presently being used to support DoD customers. It is unclear whether this gap exists because DoD support providers and customers do not realize that advanced forecast products exist and are being operationally used by the civilian climate centers, and/or because of shortcomings in DoD resources. Unlike the DoD, the civilian sector does not have this gap between capability and products.

Perhaps one way to close the DoD gap is to better inform DoD customers of the capabilities and identify their requirements for the products that can be generated by these capabilities. In a discussion of operational climate prediction at CPC, O'Lenic et al. (2007) states that "improvements in the science and production methods of LRFs [long-range forecasts] are increasingly being driven by users, who are finding an increasing number of applications, and demanding improved access to forecast information."

The challenge of closing this gap lies in the hands of the DoD meteorology and oceanography community. The majority of DoD planning occurs at two-week to intraseasonal lead times, a timeframe in which planners are not accustomed to seeing advanced climate and long range forecasting products. We need to show the mission planners the various products we can provide at long-range lead times that consistently beat standard climatology. In this thesis, we have identified several advanced products for planning operations in TC-

prone regions, including improved climatologies of TC probabilities and long-range forecasts of TC formations in the NA. Mundhenk (2009) provided similar evidence for improved products for long range planning in the WNP.

C. RECOMMENDATIONS FOR FUTURE STUDY

Though this is the third Naval Postgraduate School thesis on statistical-dynamical long-range forecasts of TC formations, there are plenty of areas that still need to be investigated further. Areas for future study include, but are not limited to the following topics and questions:

1) Is there a better NA TC data set than HURDAT? A better data set could alleviate some of the timing and placement issues with our forecast. If there is no better data set, then perhaps the DoD or NOAA should invest in one.

2) In concert with 1), climatology for TC formation is very poorly defined. A research effort to more completely and accurately define TC climatology would be very beneficial not just to military planners, but to many other government and business planners as well.

3) We have seen the propensity of our model to chase TCs that have already formed and thus produce high probabilities after TC formation. In addition to the RV2 term, is there another variable or filter that we can use to eliminate these high post-formation probabilities?

4) More investigation should be done concerning the amount of NTCI used to train the regression model. Though we tested 40, 50, 60, 80, and 100 percent NTCI, more tests need to be conducted to determine the optimal amount of NTCI.

5) Can a multiday or multi-model ensemble technique be used to produce better non-zero lead forecasts?

6) The use of a different long-range forecasting model for predicting the LSEFs might lead to more LSEFs for consideration in the training of the regression model. This would allow more choice in building the best regression model, and would reduce the potential for errors that are introduced when LSEFs needed by the regression model have to be calculated from other LSEFs rather than derived by the long-range forecast model. Further research should compare long lead forecasts from different models (e.g., models from ECMWF, advanced CFS, GFS, Goddard Space Flight Center, or the Australian Bureau of Meteorology).

LIST OF REFERENCES

Albany, 2009: Paul Roundy's Tropical Cyclone formation page. Data. [Available online at http://www.atmos.albany.edu/facstaff/roundy/tcforecast/tcforecast.html (accessed 14 June, 2009).]

Burnham, K. P., and D. R. Anderson, 2002: *Model Selection and Multimodel Inference: A Practical Information-Theoretic Approach*. 2nd ed. Springer-Verlag, 488 pp.

Camargo, S. J., 2006: Short-term climate (seasonal and intra-seasonal) prediction of tropical cyclone activity and intensity. *Proc. The Sixth WMO International Workshop on Tropical Cyclones*, San José, Costa Rica, World Meteo. Org., 493-499.

————. and A.G. Barnston, 2009: Experimental Dynamical Seasonal Forecasts of Tropical Cyclone Activity at IRI. *Wea. and Forec*. 24, 472-491.

CPC, 2007: Global Tropics Benefits/Hazards Assessment. Text and Chart. [Available online at http://www.cpc.noaa.gov/products/precip/CWlink/ghazards/ (accessed 29 April, 2009).]

Dunkerton, T. J., M. T. Montgomery, and Z. Wang, 2008: Tropical cyclogenesis in a tropical wave critical layer. *Atmos. Chem. Phys. Discuss.*, 8, 11149-11292.

Eckel, F. A., 2008: *Introduction to Ensemble Forecasting*. Naval Postgraduate School, lecture notes for MR4324 and MR4325.

Emanuel, K. A., 1989: The finite amplitude nature of tropical cyclogenesis. *J. atmos. Sci.* 46, 3431-3456.

————. 2005: *Divine Wind*. Oxford University Press, Inc. 285pp.

Frank, W. M. and P. E. Roundy, 2006: The role of tropical waves in tropical cyclogenesis. *Mon. Wea. Rev*., 134, 2397–2417.

Frank, W.M. and G. S. Young, 2007: The interannual variability of tropical cyclones. *Amer. Meteor. Soc.*., 135, 3587–3598.

Glickman, T., Ed. 2000: *Glossary of Meteorology*. 2nd ed. Amer. Meteor. Soc., 855 pp.

Gottschalck, J., Q. Zhang, W. Wang, M. L'Heureux, and P. Peng, 2008: MJO monitoring and assessment at the Climate Prediction Center and initial impressions of the CFS as an MJO forecast tool. Presentation, *NOAA CTB - COLA Joint Seminar Series*, 23 April 2008.

Gray, W. M., 1968: Global view of the origin of tropical disturbances and storms. *Mon. Wea. Rev.*, 96, 669-700.

————. 1975: Tropical cyclone genesis in the western North Pacific. U.S. Navy Tech. Rep. NEPRF TP 16-75, 66 pp.

————. 1979: Tropical cyclone origin, movement and intensity characteristics based on data compositing techniques. U.S. Navy Tech. Rep. NEPRF CR 79-06, 126 pp.

Hilldebrand, P. E, 2001: El Nino and La Nina Events and North Atlantic Tropical Cyclones. M.S. thesis, Dept. of Meteorology, Naval Postgraduate School, 108 pp.

IRI, 2009: Probability forecast for number of tropical cyclones. Chart. [Available online at http://portal.iri.columbia.edu/portal/server.pt?open=512&objID=588&PageID=0&cached=true&mode=2&userID=2 (accessed April 29, 2009).]

Kanamitsu, M., W. Ebisuzaki, J. Woollen, S.-K. Yang, J. J. Hnilo, M. Fiorino, and G. L. Potter, 2002: NCEP–DOE AMIP-II Reanalysis (R-2). *Bull. Amer. Meteor. Soc.*, 83, 1631–1643.

Leroy, A., and M. C. Wheeler, 2008: Statistical prediction of weekly tropical cyclone activity in the Southern Hemisphere. *Mon. Wea. Rev.*, 136, 3637-3654.

Madden, R.A., and P.R. Julian, 1994: Observations of the 40-50-day tropical oscillation. *Mon. Wea. Rev*., 122, 814-837.

Melton, B. F., 2007: *Sea Cobra: Admiral Halsey's Task Force and the Great Pacific Typhoon*. Globe Pequot Pr., 319 pp.

Meyer, D. W., 2007: Relationships between global warming and tropical cyclone activity in the western North Pacific. M.S. thesis, Dept. of Operations Research, Naval Postgraduate School, 163 pp.

Mundhenk, B. D., 2009: A statistical-dynamical approach to the intraseasonal prediction of tropical cyclogenesis in the western North Pacific. M.S. thesis, Dept. of Meteorology, Naval Postgraduate School, 129 pp.

NHC, 2006: Tropical Cyclone Report, Hurricane Katrina. Data. [Available online at http://www.nhc.noaa.gov/pdf/TCR-AL122005_Katrina.pdf (accessed 1 May, 2009).]

NHC, 2009: Tropical Cyclone Report, Hurricane Paloma. Data. [Available online at http://www.nhc.noaa.gov/pdf/TCR-AL172008_Paloma.pdf (accessed 1 May, 2009).]

NOAA, 2007: Tropical Cyclone Data for the North Atlantic. Data. [Available online at http://www.aoml.noaa.gov/hrd/hurdat/easyread-2008.html (accessed 12 December, 2008).]

O'Lenic, E. A., D. A. Unger, M. S. Halpert, and K. S. Pelman, 2008: Developments in operational long-range climate prediction at CPC. *Wea. Forecasting*, 23, 496-515.

Palmen, E., 1948: On the formation and structure of tropical hurricanes. *Geophysical*, 3, 26-38.

PSD, 2008: Outgoing Longwave Radiation for the North Atlantic. Chart. [Available online at http://www.esrl.noaa.gov/psd] (assessed March 24, 2009).]

Reynolds, R.W., N.A. Rayner, T.M. Smith, D.C. Stokes, and W. Wang, 2002: An improved in situ and satellite SST analysis for climate. *J. Climate*, 15, 1609-1625.

Saha, S., 2008: Documentation of operational NCEP CFS data files. [Available online at http://cfs.ncep.noaa.gov/cfs_data.pdf]. (accessed 14 May, 2009).]

————. S. Nadiga, C. Thiaw, J. Wang, W. Wang, Q. Zhang, H.M. van den Dool, H.L. Pan, S. Moorthi, D. Behringer, D. Stokes, M. Peña, S. Lord, G. White, W. Ebisuzaki, P. Peng, and P. Xie, 2006: The NCEP Climate Forecast System. *J. Climate*, 19, 3483–3517.

van den Dool, H., 2007: *Empirical Methods in Short-Term Climate Prediction*. Oxford University Press, 215 pp.

Wikipedia, 2009: Atlantic Multidecadal Oscillation. Data. [Available online at http://en.wikipedia.org/wiki/Atlantic_Multidecadal_Oscillation] (assessed March 26, 2009).]

Wilks, D. S., 2006: *Statistical Methods in the Atmospheric Sciences*. 2nd ed. Academic Press, 627 pp.

Zehr, R. M., 1992: Tropical cyclogenesis in the western north Pacific. NO Tech. Rep. NESDIS 61, 181 pp.

INITIAL DISTRIBUTION LIST

1. Defense Technical Information Center
   Ft. Belvoir, Virginia

2. Dudley Knox Library
   Naval Postgraduate School
   Monterey, California

3. Prof. Tom Murphree
   Naval Postgraduate School
   Monterey, California

4. Mr. David W. Meyer
   Naval Postgraduate School
   Monterey, California

5. Air Force Weather Technical Library
   Asheville, North Carolina